Quantitative characterization of iridescent colours in biological studies: a novel method using optical theory

Hugo Gruson, Christine Andraud, Willy Daney de Marcillac, Serge Berthier, Marianne Elias, Doris Gomez

Quantitative characterisation of iridescent colours in biological studies: a novel method using optical theory

Hugo Gruson✉[1], Christine Andraud[2], Willy Daney de Marcillac[3], Serge Berthier[3], Marianne Elias[4], and Doris Gomez[1,3]

[1]CEFE, Univ Montpellier, CNRS, Univ Paul Valéry Montpellier 3, EPHE, IRD, Montpellier, France
[2]CRC, MNHN, Ministère de la Culture et de la Communication, CNRS, Paris, France
[3]INSP, Sorbonne Université, CNRS, Paris, France
[4]ISYEB, CNRS, MNHN, EPHE, Sorbonne Université, Paris, France

Abstract

Iridescent colours are colours that change with viewing or illumination geometry. While they are widespread in many living organisms, most evolutionary studies on iridescence do not take into account their full complexity. Few studies try to precisely characterise what makes iridescent colours special: their angular dependency. Yet, it is likely that this angular dependency has biological functions and is therefore submitted to evolutionary pressures. For this reason, evolutionary biologists need a repeatable method to measure iridescent colours as well as variables to precisely quantify the angular dependency. In this study, we use a theoretical approach to propose five variables that allow to fully describe iridescent colours at every angle combination. Based on the results, we propose a new measurement protocol and statistical method to reliably characterise iridescence while minimising the required number of time-consuming measurements. We use hummingbird iridescent feathers and butterfly iridescent wings as test cases to demonstrate the strengths of this new method. We show that our method is precise enough to be potentially used at intraspecific level while being also time-efficient enough to encompass large taxonomic scales.

Keywords: iridescence, structural colours, thin-film interferences, hummingbirds, Lepidoptera, visual signals

Most interactions between organisms, whether between different species (interspecific) or different individuals of the same species (intraspecific), involve communication. Communication can have different purposes (e.g. warning, camouflage, display) and use different channels (e.g. olfactory, acoustic, visual) [1]. In particular, colour is a specific kind of communication channel that can be produced through two non-mutually exclusive mechanisms: pigmentary colours are generated by the selective absorption of some wavelengths by special molecules called pigments while structural colours are generated by the physical interaction of light with matter, causing dispersion, diffraction or interferences [2].

Among structural colours, iridescent colours change depending on the illumination or observation angle. They can be produced by interferences of light after reflection by a thin-film or multilayer structure, or diffraction on a grating. Iridescent colours are present in many taxa, and particularly widespread among bony fishes (Actinopterygii), insects, as well as some birds (see detailed review in table 3 for studies on each one of these taxa). Iridescent colours seem to be involved in many important biological processes [3] and their angular dependency is likely under selection to produce complex visual signals [4–7]. In some cases, however, angular dependency may be selected against [8]. In all those cases, the study of the evolution of iridescent colours requires a precise quantification of the angular dependency. However, the inherent physical complexity of iridescent colours has hampered the development of quantitative methods to fully describe them in the angle space.

We reviewed all studies that performed reflectance measurements of biological samples with iridescent colours produced by a multilayer or a thin-film structure in table 3. We notice two main trends: (i) many studies measure iridescence at a single fixed angle (first row in table 3). In these studies, authors generally remain cautious and warn they are not attempting to measure angle dependency. However, the multilayer or thin film producing iridescent colours may not be parallel to the sample surface [9–13], and the angle between them and the sample surface may vary between species or even between individuals of the same species [14]. Hence, even though the angle of the measuring optical fibres relative to the macroscopic is constant, the angle relative to the structures is not. This jeopardises any biological interpretation of differences between samples because the effects of many different parameters are intertwined. (ii) Other studies take measurements at multiple angles but few attempt to precisely quantify angle dependency ('Literature review' folder in ESM). Even when angle dependency is quantified, variables never stem from a theoretical approach, which leads to a large diversity of custom variables for each author. This heterogeneity in the meth-

✉hugo.gruson@normalesup.org

ods, variable naming, and sign conventions have likely hindered the spread of new concepts and results among researchers working on iridescence in living organisms.

Osorio and Ham [15] and Meadows et al. [16] started to address this heterogeneity in measurement methods and advocated for the use of a goniometer to reliably measure colour in a controlled angle configuration. However, they did not propose a detailed protocol or statistical tools to study angular dependency. Here, we use the optical laws that govern iridescence to propose a set of parameters to characterise angle dependency of brightness, hue and saturation of iridescent colours. Next, we confirm the validity of these equations for complex biological structures using two highly different groups of organisms well-known for their iridescent colours: Trochilidae (hummingbirds) and Lepidoptera (i. e., butterflies and moths), including the iconic *Morpho* butterflies that harbour large wings with bright iridescent blue colours. The standard framework we propose here makes iridescent colours comparable across taxa and across studies, opening up new perspectives in the study of their biological functions.

1 Model

1.1 Choice of colour variables

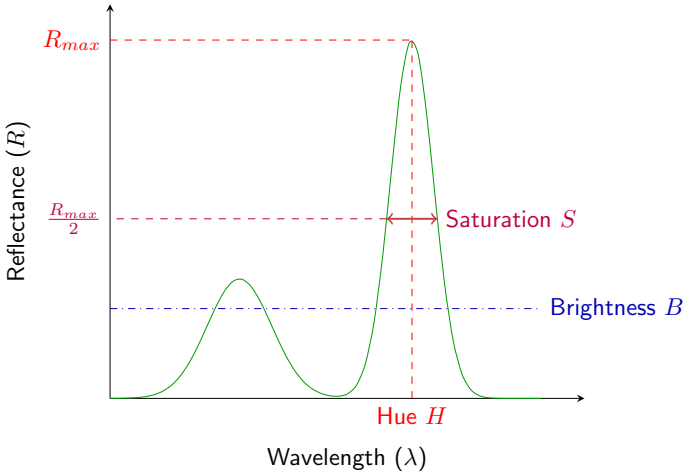

Figure 1. Graphical representation of the variables we used for hue H (wavelength at peak reflectance R_{max}; called H_1 in Montgomerie [17]), brightness B (average of reflectance over the wavelength range of interest; B_2 in [17]) and saturation S (full width at half maximum: no equivalent in [17]).

Since we want to produce a general method that does not depend on any specific vision system, we use variables directly derived from spectra, without computing vision models. We define brightness B as the average reflectance over a range between the minimal (λ_{min}) and maximal (λ_{max}) wavelengths (B_2 in Montgomerie [17]), saturation S as the full width at half maximum reflectance and hue H as the wavelength at which reflectance is maximal (H_1 in Montgomerie [17]). These three variables are represented in fig. 1 and are the most common measures of brightness, hue and saturation in studies about iridescence (see literature review in ESM).

1.2 Assumptions and equations

Our method relies on three assumptions that greatly simplify the equations for brightness, hue and saturation in the angle space. See Appendix 1 for mathematical proofs of the equations and the role of each one of these assumptions:

1. Small angles ($\leq$ 30°). Outside of this range, the signal due to iridescence is often very low and all that remains is the effect of the underlying pigments, which can be measured through traditional methods. For all thin films, and in some multilayers (depending on chemical composition), it is possible to consider angles up to 45°, as illustrated in ESM. This may help producing more repeatable parameter estimates. For instance, a 45° angle can correspond to a viewer standing next to the viewed iridescent patch illuminated from above. Many previous studies have in this way mimicked the position of the bird relative to the sun in their measurements [7, 14, 16, 18–20].

2. The orientation of the layers within the multilayer structure is affected by Gaussian noise. Many developmental processes are controlled by a large array of independent factors of small effect each, causing subsequent errors to often be Gaussian (due to the central limit theorem). This assumption is also empirically supported by the results of Gur et al. [21] who looked at the orientation of guanine crystals in neon tetra fishes (*Paracheirodon innesi*) using wide-angle X-ray scattering (WAXS). Fitting a Cauchy distribution (fatter tail distribution) instead of a Gaussian distribution yields similar values of parameter estimates. For simplicity, we here only present the results with Gaussian noise.

3. Multilayers are ideal, i. e. the optical thickness (layer thickness times optical index) of each layer is constant: $n_1 e_1 = n_2 e_2$. This is a common assumption [9, 22–29] which is thought to be valid for most animal reflectors [30] because it produces the brightest and most saturated signals with a minimal number of layers (but see Schultz and Rankin [31] and Parker et al. [32] for beetles, Kinoshita et al. [33] for neon tetra).

This set of assumptions allows us to formally derive simple analytic expressions of brightness B, hue H and saturation S (fig. 1) in the angle space $(\Phi_{\text{inc}}, \Phi_{\text{col}})$. All variables used in this study with their notations and their possible values are listed in table 1 and illustrated whenever possible on fig. 2.

$$B(\Phi_{\text{inc}}, \Phi_{\text{col}}) = B_{\text{max}} \exp - \frac{\left(\frac{\Phi_{\text{inc}} - \Phi_{\text{col}}}{2} - t\right)^2}{2\gamma_B^2} \qquad \text{(8 bis)}$$

$$H(\Phi_{\text{inc}}, \Phi_{\text{col}}) = H_{\text{max}} \cos(\gamma_H \frac{\Phi_{\text{inc}} + \Phi_{\text{col}}}{2}) \qquad \text{(18 bis)}$$

$$S(\Phi_{\text{inc}}, \Phi_{\text{col}}) = S_{\text{max}} \qquad (1)$$

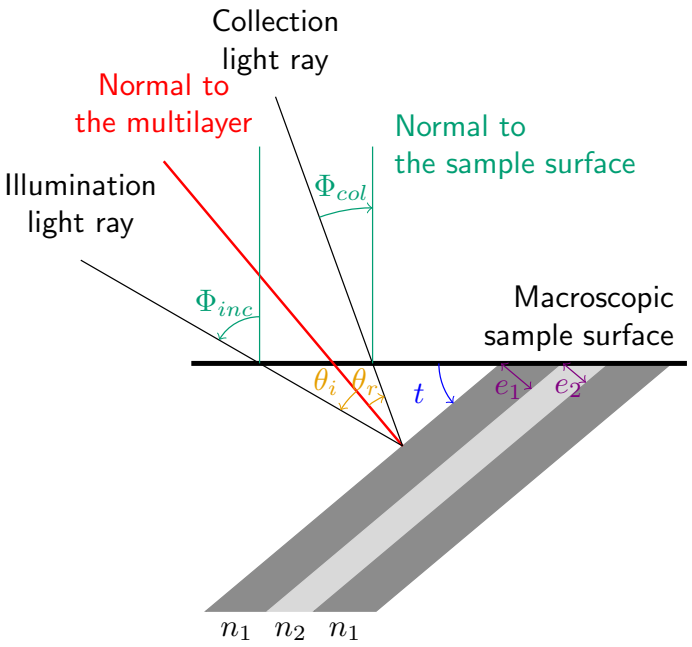

Figure 2. Schematic representation of a tilted multilayer (angle between the multilayer and the sample surface or tilt $t = 40°$) and incoming and reflected light rays relative to the multilayer structure (with angles θ_i and θ_r respectively) and relative to the sample surface (with angle Φ_{inc} and Φ_{col} respectively). There is a relationship involving the tilt t between angles relative to the multilayer structure (θ_i and θ_r) and angles relative to the sample surface (Φ_{inc} and Φ_{col}): $\theta_i = \Phi_{\text{inc}} - t$ and $\theta_r = \Phi_{\text{col}} + t$. The positive direction for each angle is figured by an arrowhead. The multilayer is composed of an alternance of two layers characterised by the optical indices n_1 and n_2 and their thicknesses e_1 and e_2. A schematic representation at a different scale, focusing on the goniometer is available in ESM.

Hereafter, we focus on brightness B and hue H because saturation S is constant no matter the angle configuration. The brightness $B(\Phi_{\text{inc}}, \Phi_{\text{col}})$ in the angle space is entirely defined by three parameters: B_{max}, t and γ_B. The tilt t is the angle between the multilayer structure and the sample surface (as illustrated in fig. 2). B_{max} is the maximum reflectance produced by the multilayer of thin-film structure, reached when the fibres are placed in a symmetrical configuration relative to the normal of the multilayer. γ_B is the parameter quantifying the disorder in the alignment of the multilayer structure. This disorder in the structure results in a reflected signal that is not purely specular but instead contains a diffuse component, meaning it can be seen at multiple angle configurations. For this reason, from a macroscopic point of view, γ_B is correlated with the angular dependency of brightness. Earlier studies used a binary classification of iridescent colours depending on the angle range at which the colour was visible ('diffuse/directional' in Osorio and Ham [15], 'wide-angle/flashing' in Huxley [34], 'limited view' of Vukusic et al. [35]). This classification is positively correlated with $\frac{1}{\gamma_B}$. The hue $H(\Phi_{\text{inc}}, \Phi_{\text{col}})$ in the angle space is defined by two parameters: H_{max} which is the hue at coincident geometry (when using a bifurcated probe for example) and γ_H is the angular dependency of hue.

The variations of brightness and hue in the angle space, according to eq. (8) and eq. (18) respectively are represented in fig. 3.

1.3 Angle and notation conventions

In the rest of this study, we measure the incoming light ray angles (θ_i and Φ_{inc}) counter-clockwise and the outgoing light ray angles (θ_r and Φ_{col}) clockwise. For both incoming and outgoing angles, the origin is the normal to the structures (θ_i and θ_r) or the normal to the sample (Φ_{inc} and Φ_{col}). These conventions are represented on fig. 2 where the direction of the arrows on angles represent the positive direction. The tilt t corresponds to the angle between the multilayer and the surface of the sample and is defined as $t = \Phi_{\text{inc}} - \theta_i = \theta_r - \Phi_{\text{col}}$ (see Appendix 1 for more details about t). In other words, t is positive when the multilayer is tilted towards the illumination and negative otherwise (i.e. t is measured clockwise).

2 Methods

2.1 Study system: hummingbirds and butterflies

We used hummingbirds and butterflies (more precisely some *Morpho* and *Papilio* species) as study systems. Hummingbirds make an ideal example to test our framework for numerous reasons. First, they belong to a speciose family where all species are iridescent [36], which allows us to work on a large number of species that diverged fairly recently [37]. Upon visual examination, they display highly different types of iridescent colours, with either 'diffuse' (usually on dorsal patches) 'directional' (usually on facial or ventral patches) iridescence (*sensu* Osorio and Ham [15]). In addition, many species have highly tilted multilayers, providing a good test case to estimate the tilt t [15, 16]. Finally, most species are available in large numbers in museum collections. We obtained the authorisation from the Muséum National d'Histoire Naturelle to carefully cut feathers using surgical scissors. We selected one male from 36 species, evenly distributed across the phylogeny, from which we took feathers on two patches, one diffuse and one directional (*sensu* Osorio and Ham [15]).

Because the exclusive use of hummingbirds as a test taxon for a new method has been criticised in previous studies [38], we also test our method on a very different group: butterflies. Butterflies are phylogenetically distant from birds and have different structures producing iridescence. For these reasons, the fact our method works in both taxa is a compelling argument for its universality. We used 17 butterfly species known to have multilayer structures [39, 40]. The full list of species we used for our measurements is available in ESM, for both hummingbirds and butterflies.

The method presented is also valid for whole specimens (whole birds instead of plucked feathers for example). We nonetheless opted for the use of single feathers to maximise repeatability. Indeed, the precision of the goniometer measurements relies on the fact that the sample is precisely located at the centre of rotation of both fibres, which is more difficult to ensure for whole specimens.

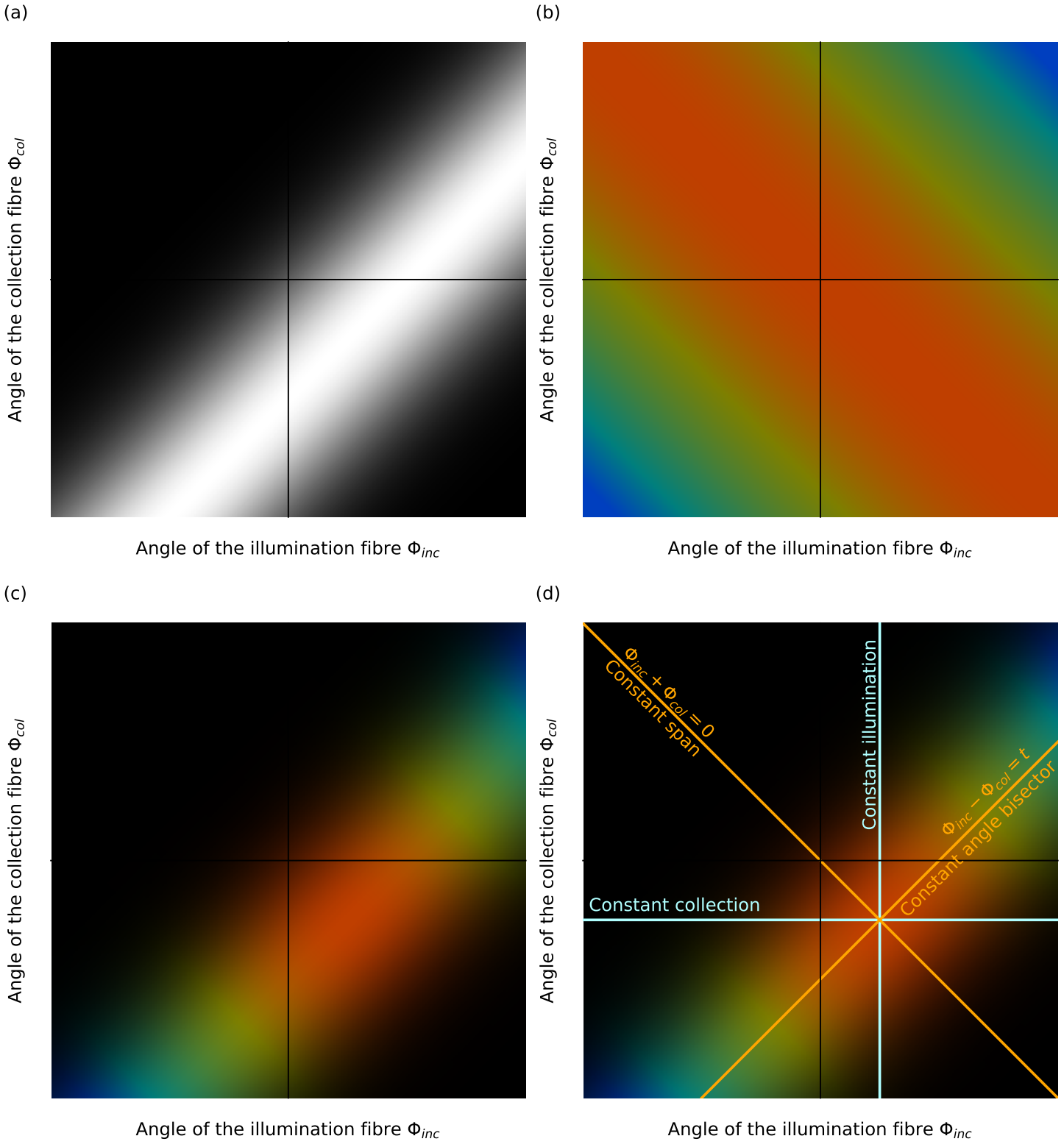

Figure 3. Colour variables ((a): brightness; (b): hue; (c) and (d): hue & brightness) of an iridescent multilayer (with tilt $t \neq 0$) in the angle space relative to the sample surface $(\Phi_{\text{inc}}, \Phi_{\text{col}})$. The colour lines in (d) indicate alternative bases: the angle space relative to the multilayer structure (θ_i, θ_r) in blue and $(\Phi_{\text{inc}} + \Phi_{\text{col}} = 0, \Phi_{\text{inc}} - \Phi_{\text{col}} = t)$ in orange and illustrates the terms 'constant illumination', 'constant collection', 'constant angle bisector' and 'constant span' used in table 3 and throughout this article.

Symbol	Range	Meaning
θ_i	$\left[-\frac{\pi}{2};\frac{\pi}{2}\right]$	Incident light angle relative to the multilayer
θ_r	$\left[-\frac{\pi}{2};\frac{\pi}{2}\right]$	Reflected light angle relative to the multilayer
θ_1	$\left[0;\frac{\pi}{2}\right]$	Angle between the incident ray and the interface between layers 1 and 2
θ_2	$\left[0;\frac{\pi}{2}\right]$	Angle between the transmitted ray and the interface between layers 1 and 2 Angle between the incident ray and the interface between layers 2 and 1
m	$\mathbb{N}$	Interference order/rank
B	$\mathbb{R}^+$	Brightness at a given configuration
H	$[\lambda_{\mathsf{min}};\lambda_{\mathsf{max}}]$	Hue at a given angle configuration
S	$\mathbb{R}^+$	Saturation at a given angle configuration
B_{max}	$\mathbb{R}^+$	Maximal brightness value (achieved for specular position)
t	$\left[-\frac{\pi}{2};\frac{\pi}{2}\right]$	Angle between the multilayer surface and the sample surface (=tilt)
γ_B	$\mathbb{R}^+$	Disorder of the layer alignment in the multilayer/Angular dependency of brightness
H_{max}	$[\lambda_{\mathsf{min}};\lambda_{\mathsf{max}}]$	Maximal hue value (achieved at normal incidence geometry)
γ_H	$\mathbb{R}^+$	Angular dependency of hue
n	$\mathbb{C}$	Optical index of the material
e	$\mathbb{R}^+$	Thickness of the layer(s)
Φ_{inc}	$\left[-\frac{\pi}{2};\frac{\pi}{2}\right]$	Angle between incidence fibre and sample surface (measured counterclockwise)
Φ_{col}	$\left[-\frac{\pi}{2};\frac{\pi}{2}\right]$	Angle between collection fibre and sample surface (measured clockwise)
cst	$\mathbb{R}$	Used to denote a constant whose value is not important for the calculations

Table 1. List of parameters used in this study, with their domains of definition and their meanings.

2.2 Reflectance measurements

We measured reflectance at various angles using a purpose-built goniometer, following the recommendations of Meadows et al. [16]. The light emitted by a Xenon lamp (300 W) over the 300 nm to 700 nm range of wavelengths to which birds are sensitive [41] was brought to the sample through an illuminating UV-VIS optical fibre collimated to get a 1 mm light spot at normal illumination. Light reflected by the sample was then collected by a second identical collimated optical fibre and conducted toward an Oceanoptics USB4000 spectrophotometer. This setup allows for a precise independent rotation of the illumination and the collection fibres, necessary for the measurements of iridescent colours.

Our previous mathematical exploration revealed that hue is constant along the $\Phi_{\mathsf{inc}}+\Phi_{\mathsf{col}}=\mathsf{cst}$ line ('constant span') and brightness along the $\Phi_{\mathsf{inc}}-\Phi_{\mathsf{col}}=\mathsf{cst}$ line ('constant angle bisector'), as illustrated in fig. 3. We thus only need to take measurements in two orthogonal directions: in the direction $\Phi_{\mathsf{inc}}-\Phi_{\mathsf{col}}=\mathsf{cst}$ to quantify hue variation and in the direction $\Phi_{\mathsf{inc}}+\Phi_{\mathsf{col}}=\mathsf{cst}$ to quantify brightness variations. This will allow us to infer all parameters controlling hue and brightness, and therefore to potentially compute all values of hue and brightness in the entire angle space $(\Phi_{\mathsf{inc}},\Phi_{\mathsf{col}})$.

The shape and size of the light spot on the sample depends on the position of the illuminating fibre relatively to the sample. As the angle of illumination θ_i increases, the light spot becomes more and more elongated, according to a θ_i cosine function. This means the amount of light received by the spectrometer decreases when θ_i increases, independently of sample characteristics. This can also be empirically observed by taking measurements of the white reference (which is a Lambertian surface, i. e., reflectance does not depend on the angle) at different angles. To control for this, we took white reference measurements at several angle configurations (detailed in the protocol below). The white standard for this study was an Avantes reference tile WS-2. Because this is a diffuse (Lambertian) white reference and because some iridescent colours are very directional (i.e., all reflected light is focused in a single direction), it is expected to sometimes get values of brightness that can be over 100 %.

The detailed protocol we used for our measurements is similar to Waldron et al. [20] and inspired from Osorio and Ham [15] and Meadows et al. [16]. A detailed walkthrough of the measurement protocol is presented in box 1.

We repeated each measurement twice, on different days, by two different experimenters for hummingbirds and butterflies. We performed statistical analyses after the completion of the measurement session to prevent experimenter bias.

2.3 Statistical analyses

As explained in the previous section, the angle configuration changes the shape of the light spot and thus the total possible amount of light collected by the collection fibre. To address this issue, we first pre-processed spectra to normalise count data using the appropriate reference white spectrum (script available in ESM). Resulting `csv` files were then imported in `pavo` R package [42]. Hue values were discarded (i.e. converted to `NA`) when brightness was lower than 8.5 % because hue is not defined for black colours.

Iridescence parameters can be estimated using various methods, including least squares optimisation and Bayesian non linear regression. We used a least squares optimisation as it is more common in biological sciences. We tested the Bayesian approach as well but it returned similar results and it is therefore not presented here.

We used two indices to estimate the variability of the parameters resulting from our method: (i) Relative standard deviation (RSD, also called coefficient of variation or

Box 1: Measurement protocol

1. Move one of the two fibres of the goniometer to find the position where you get a signal of maximal intensity. This position depends on the tilt t of the multilayer and is therefore different for every sample. Once this is done, this means the angle bisector of the two fibres is close to the normal to the multilayer structure (red line in fig. 2).
2. While keeping the same angle bisector, take measurements at different angular spans (orange line $\Phi_{inc} - \Phi_{col} = t$ in fig. 3d). These measurements will be used to estimate hue parameters. To have a sample size large enough for reliable estimation and to stay at small angles, we recommend measurements at $(\Phi_{inc}, \Phi_{col}) \in \{(t + 5°, t + 5°), (t + 10°, t + 10°), (t + 15°, t + 15°), (t + 20°, t + 20°), (t + 25°, t + 25°)\}$.
3. Take measurements while keeping the angular span between the two fibres constant (for example $\Phi_{col} - \Phi_{inc} = 20°$) and moving the angle bisector (if you cannot do this, because for example, one of your fibres is not mobile, see section 6.2). This will be used to estimate parameters related to brightness. We recommend 3 measurements on each side of the supposed normal to the multilayer structure (7 measurements in total) and a span of 20°: $(\Phi_{inc}, \Phi_{col}) \in \{(t - 5°, t + 25°), (t°, t + 20°), (t + 5°, t + 15°), (t + 10°, t + 10°), (t + 15°, t + 5°), (t + 20°, t + 0°), (t + 25°, t - 5°)\}$. Depending on how directional your sample is, it may be needed to increase the resolution of the measurement grid and only move the angle bisector of 2.5° or 5° at each step.
4. Take white reference measurements with the same angular spans as before but using the normal to the goniometer as angle bisector (same measurements as in 2 but with $t = 0°$). If you have followed our advice for measurements, you should now take white measurements at $(\Phi_{inc}, \Phi_{col}) \in \{(5°, 5°), (10°, 10°), (15°, 15°), (20°, 20°), (25°, 25°), (30°, 30°)\}$.
5. Take white reference measurements with a constant span but various angle bisectors (same measurements as in 3 but with $t = 0°$). If you have followed our advice of 3 measurements on each side to the supposed normal to the multilayer structure and a span of 20°, you should now take white measurement at $(\Phi_{inc}, \Phi_{col}) \in \{(-5°, 25°), (0°, 20°), (5°, 15°), (10°, 10°), (15°, 5°), (20°, 0°), (25°, -5°)\}$

CV) as the standard deviation divided by the absolute value of the mean. (Absolute) standard deviation SD is a common measure of the noise in a dataset. RSD is a way to quantify the signal-to-noise ratio. Because it is normalised by the mean value of the parameter, it is dimensionless and can be compared between parameters. It represents the precision of the experimental and statistical framework and does not depend on the sample population.(ii) Repeatability as the intra-class coefficient (ICC) computed with the `rptR` package [43]. ICC assesses whether the method allows to discriminate individual samples among the population by comparing intra- and inter-samples standard deviation. ICC is therefore highly dependent on the sample population and on the biological question.

RSD and ICC complement each other. A very precise method can still lead to non-repeatable measurements is there is no variability in the population. Conversely, a coarse method can work well enough to discriminate between samples and be repeatable if the variability between samples is high.

3 Results and discussion

Spectra from measurement along the 'constant span' ($\Phi_{inc} + \Phi_{col} = 20°$) and 'constant angle bisector' ($\Phi_{inc} - \Phi_{col} = cst$) lines after correction by the appropriate white reference are displayed in fig. 4 for the iridescent blue of the breast of the hummingbird *Heliomaster furcifer*. We also show values of hue H and brightness B along these two measurement lines as well as the result from parameters estimation.

3.1 Relative error and repeatability

Variability and repeatability results are summarised in table 2. We find low values of RSD for hue-related variables for both hummingbirds and butterflies, indicating that our framework provides precise estimations of parameters. For brightness-related parameters, RSD is higher, as it is usually the case, even for non-iridescent colours [44–46]. Despite relatively high RSD, all values for brightness remain repeatable, expected tilt t for butterflies because of a low inter-species variability, as demonstrated by the low value of standard deviation SD.

3.2 Correlation between parameters

3.2.1 Correlation between B_{max} and γ_B

Madsen et al. [14] noticed a negative relationship between brightness angular dependency and maximum brightness. From an evolutionary point of view, this means there is a trade-off between the signal brightness at a given angle and the range of angle at which it is not black (i.e. directionality *sensu* Osorio and Ham [15]).

This correlation can also be proved theoretically. Indeed, the total energy of light that is reflected by the sample cannot exceed the received light energy. In other words, if absorption is similar across samples, the total

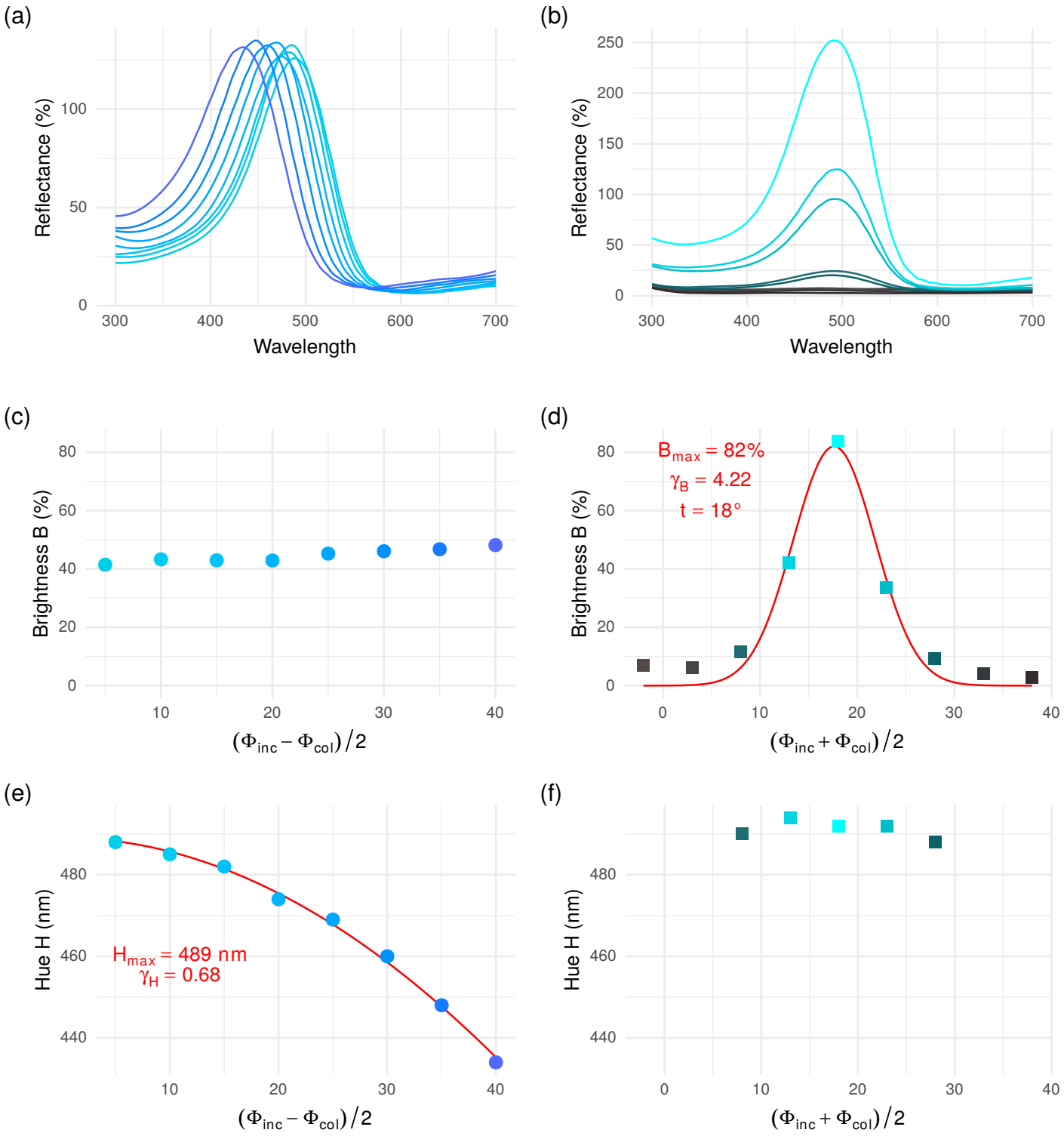

Figure 4. Spectra (top row) and corresponding values of brightness (middle row) and hue (bottom row) at different angle configurations for the breast patch of the hummingbird *Heliomaster furcifer* along the $\Phi_{inc} - \Phi_{col} = cst$ (left column; data points with round shape) and $\Phi_{inc} + \Phi_{col} = cst$ (right column; data point with square shape) lines. Colours correspond to the conversion of the spectra in human vision using the CIE10 visual system. As expected, brightness is constant when $\Phi_{inc} - \Phi_{col} = cst$ and has a Gaussian shape when $\Phi_{inc} + \Phi_{col} = cst$. Conversely, hue has a cosine shape wen $\Phi_{inc} - \Phi_{col} = cst$ and is constant when $\Phi_{inc} + \Phi_{col} = cst$. The red lines correspond to the fit of the functions after parameters estimation, with the values of the parameters. The R script to produce this figure is available in ESM.

Taxon	Variable	Param.	mean	SD	RSD (%)	ICC	p (likel.)	p (perm.)
Hummingbirds	Brightness	B_{max}	36.60	47.54	14.79	0.947	<0.0001	0.001
		t	14.61	18.21	7.428	0.968	<0.0001	0.001
		γ_B	13.67	7.85	11.19	0.875	0.0009	0.002
	Hue	H_{max}	556.80	65.66	0.3004	0.997	<0.0001	0.001
		γ_H	0.64	0.18	2.281	0.689	0.028	0.098
Butterflies	Brightness	B_{max}	148.80	99.78	6.91	0.936	<0.0001	0.001
		t	2.94	4.83	32.96	0.268	0.18	0.098
		γ_B	5.35	5.12	4.76	0.769	<0.0001	0.004
	Hue	H_{max}	492.69	27.87	0.2484	0.993	<0.0001	0.001
		γ_H	0.73	0.14	2.993	0.853	<0.0001	0.001

Table 2. Repeatability (intra-class coefficient ICC with likelihood ratio and permutation p-values) and standard deviations (standard deviation SD and relative standard deviation RSD) of iridescence parameters for hummingbird and butterflies.

brightness reflected in all directions is constant across samples:

$$\iint B(\Phi_{\text{inc}}, \Phi_{\text{col}})\, d\Phi_{\text{inc}}\, d\Phi_{\text{col}} = \text{cst} \tag{2}$$

The value of this double integral is known ($B(\Phi_{\text{inc}}, \Phi_{\text{col}})$ is a bivariate Gaussian function) and when we compute it, we find:

$$B_{\text{max}}\sqrt{2\pi\gamma_B^2} = \text{cst} \tag{3}$$

$$B_{\text{max}} \propto \frac{1}{\gamma_B} \tag{4}$$

We indeed find a positive correlation between B_{max} and $\frac{1}{\gamma_B}$ in the empirical data ($F = 147.0742$, $df = 1$, $p < 0.0001$), illustrated in fig. 5. We also notice an effect of the taxon (butterflies or hummingbirds) on the slope of the correlation ($F(1) = 8.3198$, $p = 0.0057$). Because the link between B_{max} and $\frac{1}{\gamma_B}$ was proven when ignoring absorption (eq. (4)), this may suggest that absorption is higher in hummingbirds than in butterflies.

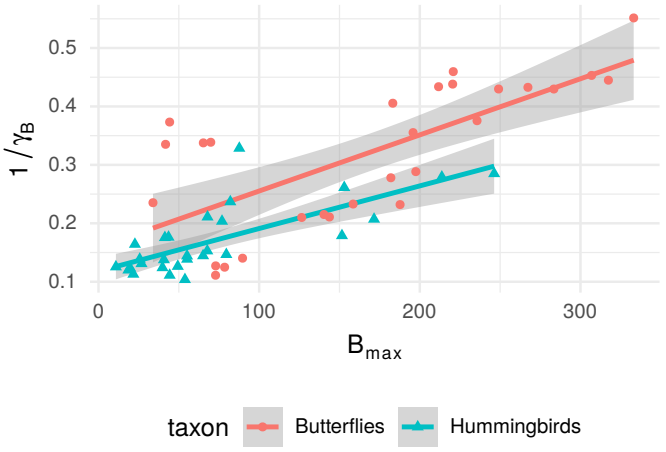

Figure 5. Correlation between B_{max} and directionality $1/\gamma_B$. The dots are the data points. The lines show the result of the linear model.

3.2.2 Correlation between angular dependency for hue γ_H and and other parameters

Osorio and Ham [15] found that γ_H and γ_B are negatively correlated among 15 bird species from different families. We do not find support for such correlation for either the hummingbirds or the butterflies ($F(1) = 3.1994$, $p = 0.074$, figure in ESM). Additionally, as discussed later in section 6.3.2, many studies use variables that are correlated to H_{max} to quantify hue angular dependence. On the contrary, we find that the parameters used in our method, H_{max} and γ_H are not correlated ($F(1) = 0.5167$, $p = 0.47$, figure in ESM).

4 Conclusion

Using both a theoretical and an experimental approach we find that hue and brightness can be easily characterised for all angle configurations using a set of 5 parameters (H_{max} and γ_H for hue; B_{max}, t and γ_B for brightness). Additionally, we show that a relatively small number of measurements is sufficient to reliably estimate these parameter values. This is made possible by the fact that hue is constant when the angular span between the two fibres remains constant ($\Phi_{\text{inc}} - \Phi_{\text{col}} = \text{cst}$), and that brightness is constant for small angles as long as the angle bisector remains in the same position ($\Phi_{\text{inc}} + \Phi_{\text{col}} = \text{cst}$) (as illustrated in fig. 3 and fig. 4). These properties have been previously noticed empirically for hue H_1 by Osorio and Ham [15] on 15 bird species sampled from different families and Meadows et al. [16] on *Calypte anna*. Without being formalized, it had been illustrated for brightness in Eliason and Shawkey [47] and Stavenga et al. [48] on B_3, Stavenga et al. [49] for B_1.

Our contribution unlocks new perspectives for studies on iridescent colours, such as the evolution of complex visual signals leveraging angular dependency properties of iridescent colours.

The proofs for the equation in this article are based on the multilayer theory. However, it is possible that parts of it may work for iridescence from diffraction gratings. Future studies should aim at integrating iridescence

from diffraction into our framework. This would allow for a standard set of variables to describe iridescence, no matter its physical origin. Further investigation is also required to assess whether it is possible to relax some of the assumptions made in the manuscript under certain conditions.

Data accessibility Data used in this study as well as scripts to apply the described method are available at `https://doi.org/10.5281/zenodo.1412735`.

Competing interests The authors declare no competing interests.

Author contributions HG conducted the study (model construction, data analysis) and wrote the first version of this manuscript. HG performed measurements on hummingbirds and DG on butterflies. WDdM designed and built the goniometer. CA, DG, ME, SB contributed to the design of the goniometer. CA, DG and WDdM helped with measurement protocol. DG and ME participated in the discussion for biological significance and pitfalls. All authors contributed to the final version of this article.

Acknowledgements We are grateful to C. Doutrelant and two anonymous reviewers for their valuable comments on this manuscript. We would also like to thank the Muséum National d'Histoire Naturelle and in particular J. Fuchs, P. Boussès, and A. Previato for letting us sample feathers from museum hummingbird specimens, as well as V. Debat for lending us *Morpho* specimens to explore *Morpho* iridescence. Finally, we thank the Living Light conference organisers for putting together this special issue on structural colours in living organisms.

5 Appendix 1: mathematical proof of the equations

5.1 Brightness B in the angle space $(\Phi_{\text{inc}}, \Phi_{\text{col}})$

For a perfectly regular multilayer, all the reflected signal is focused in the specular direction, at an angle θ_r equal to the incident angle θ_i. The brightness B is proportional to the reflected signal intensity, meaning:

$$B(\theta_i, \theta_r) = \begin{cases} B(\theta_i) & \text{if } \theta_i = \theta_r \\ 0 & \text{if } \theta_i \neq \theta_r \end{cases} \tag{5}$$

where $B(\theta_i)$ is defined by the Fresnel factor in the case of a thin-film structure (equation and R code to compute the Fresnel factor available in ESM). However, because we are dealing with small angles (hypothesis 1), we can approximate $B(\theta_i)$ to a constant B_{max} (as illustrated in ESM):

$$B(\theta_i, \theta_r) \approx \begin{cases} B_{\text{max}} & \text{if } \theta_i = \theta_r \\ 0 & \text{if } \theta_i \neq \theta_r \end{cases} \tag{6}$$

But because biological structures are not entirely flat, and because the different layers of the multilayer structure are not perfectly aligned, there is also some amount of light reflected outside of the specular reflection (often referred as diffuse reflection). We thus assume a Gaussian decay of the brightness B around the specular position $\theta_i = \theta_r$ (assumption 2), controlled by a parameter γ_B related to the disorder of the multilayer:

$$B(\theta_i, \theta_r) \approx B_{\text{max}} \exp -\frac{\left(\frac{\theta_i - \theta_r}{2}\right)^2}{2\gamma_B^2} \tag{7}$$

In the case of an perfectly regular multilayer with no disorder, we have $\gamma_B = 0$ and we find eq. (6). Conversely, if $\gamma_B = +\infty$, the value of brightness is the same for all angle configurations, which means we are dealing with a Lambertian surface.

Additionally, the multilayer structure is not always parallel to the sample surface. It is the case for example for hummingbirds included in this study, as well as for *Morpho* butterflies [9],for the rainbow stag beetle, *Phalacrognathus muelleri*, structures described in Edo et al. [10], 6 pierid butterflies in Pirih et al. [11], 10 species of butterflies in Wickham et al. [12], and for 6 species of *Heliconius* butterflies in Parnell et al. [13]). So the illuminating angle Φ_{inc} and the collection Φ_{col} at the macroscopic scale do not necessarily match θ_i and θ_r (as illustrated in fig. 2). If we denote t the angle between the multilayer surface and the macroscopic sample surface (called tilt hereafter, as in Madsen et al. [14] and Osorio and Ham [15]), we get:

$$B(\Phi_{\text{inc}}, \Phi_{\text{col}}) \approx B_{\text{max}} \exp -\frac{\left(\frac{\Phi_{\text{inc}} - \Phi_{\text{col}}}{2} - t\right)^2}{2\gamma_B^2} \tag{8}$$

Using eq. (8), we only have 3 parameters (B_{max}, t and γ_B) to estimate to be able to reconstruct all values of brightness B in the angle space defined by $(\Phi_{\text{inc}}, \Phi_{\text{col}})$. The resulting brightness in this space in plotted in fig. 3.

5.2 Hue H in the angle space $(\Phi_{\text{inc}}, \Phi_{\text{col}})$

We defined the hue H as the wavelength for which reflectance is maximal. In the context of interferences, it is therefore the wavelength for which reflected light interferes constructively. For a regular multilayer, this happens when:

$$mH(\theta_1, \theta_2) = 2(n_1 e_1 \cos\theta_1 + n_2 e_2 \cos\theta_2) \tag{9}$$

where m is an integer (interference order), θ_1 is the angle between the incident light ray and the multilayer structure at the interface between layer 1 and 2, θ_2 is the angle between the transmitted ray after going through the first interface between layers 1 and 2 and the multilayer structure, n_1 and n_2 are the optical indices of the layers, and e_1 and e_2 the thickness of the layers. The product $n_1 e_1$ and $n_2 e_2$ is often called optical thickness of the layers 1 and 2 (respectively).

The relationship between θ_1 and θ_2 is given by Snell's law:

$$n_1 \sin\theta_1 = n_2 \sin\theta_2 \tag{10}$$

Because $\theta_1 \in [0; \frac{\pi}{2}]$, hue H increases when angle θ_1 decreases according to eq. (9). This means a maximum value for hue H_{max} is achieved when $\theta_1 = 0$ (in this case $\theta_2 = 0$ as well because of Snell's law; eq. (10)):

$$mH_{\text{max}} = 2(n_1 e_1 + n_2 e_2) \tag{11}$$

We can replace $n_1 e_1$ and $n_2 e_2$ in eq. (9) using eq. (11):

$$mH(\theta_1,\theta_2) = mH_{\text{max}}(\cos\theta_1 + \cos\theta_2) - 2(n_1 e_1 \cos\theta_2 + n_2 e_2 \cos\theta_1) \quad (12)$$

By adding eq. (12) and eq. (9), we get:

$$2mH(\theta_1,\theta_2) = mH_{\text{max}}(\cos\theta_1 + \cos\theta_2) + 2(\cos\theta_1 - \cos\theta_2)(n_1 e_1 - n_2 e_2) \quad (13)$$

We consider here the case of an ideal multilayer, meaning that $n_1 e_1 = n_2 e_2$ (assumption 3). This allows us to simplify eq. (13) into:

$$H(\theta_1,\theta_2) = H_{\text{max}} \frac{\cos\theta_1 + \cos\theta_2}{2} \quad (14)$$

Because we are working with small angles (assumption 1), Snell's law (eq. (10)) can be approximated by:

$$\theta_2 \approx \frac{n_1}{n_2}\theta_1 \quad (15)$$

$$H(\theta_1,\theta_2) \approx H_{\text{max}} \frac{\cos\theta_1 + \cos\frac{n_1}{n_2}\theta_1}{2} \quad (16)$$

For small angles (assumption 1), this sum of cosine functions can be approximated by a single cosine function with twice the amplitude (numerical proof in ESM):

$$H(\theta_1,\theta_2) \approx H_{\text{max}} \cos\gamma_H \theta_1 \quad (17)$$

where $\gamma_H \approx \sqrt{\frac{1+\left(\frac{n_1}{n_2}\right)^2}{2}}$ (after identification of the coefficients of the second-order Taylor series expansions in eq. (16) and eq. (17)).

This reasoning is valid for ideal thin film structures and multilayers and tells what happens at the specular position. But as explained in the previous section, biological structures are noisy and there is signal outside the specular position. As previously, if there is signal, this means that there is a multilayer for which the position of the fibres is specular. And in this case, we can apply eq. (17) as well.

$$H(\Phi_{\text{inc}},\Phi_{\text{col}}) = H_{\text{max}} \cos\left(\gamma_H \frac{\Phi_{\text{inc}} + \Phi_{\text{col}}}{2}\right) \quad (18)$$

We only need two parameters (H_{max} and γ_H) to plot all hue values in the angle space $(\Phi_{\text{inc}},\Phi_{\text{col}})$ as in fig. 3. In the case of non-iridescent colours, we have $\gamma_H = 0$.

5.3 Saturation S in the angle space $(\Phi_{\text{inc}},\Phi_{\text{col}})$

5.3.1 Along the 'constant span' direction ($\Phi_{\text{inc}} + \Phi_{\text{col}} =$ cst)

We know that along the $\Phi_{\text{inc}} + \Phi_{\text{col}} =$ cst direction (constant span), hue is constant (as shown in eq. (18) and fig. 3b). Using a similar reasoning as in section 5.1, we find that the reflectance R for a wavelength λ at a given angle configuration $(\Phi_{\text{inc}},\Phi_{\text{col}})$ is given by:

$$R(\Phi_{\text{inc}},\Phi_{\text{col}},\lambda) = R_{bisector}(\lambda) \exp -\frac{\left(\frac{\Phi_{\text{inc}}-\Phi_{\text{col}}}{2} - t\right)^2}{2\gamma_B^2} \quad (19)$$

This means that reflectance spectra at all angle configurations along the 'constant span' axis ($\Phi_{\text{inc}} + \Phi_{\text{col}} =$ cst) can be derived by scaling of the spectrum at another angle configuration.

The saturation $S(\Phi_{\text{inc}},\Phi_{\text{col}})$ is defined as the full width at half maximum of the reflectance spectrum $R(\Phi_{\text{inc}},\Phi_{\text{col}},\lambda)$. Let us call R the reflectance spectrum at a given angle configuration $(\Phi_{\text{inc}}^{pos1},\Phi_{\text{col}}^{pos1})$. Then the saturation S at this configuration is:

$$\begin{cases} S = \lambda_1 - \lambda_2 \\ R(\lambda_1) = R(\lambda_2) = \frac{R_{\text{max}}}{2} \\ \lambda_1 > \lambda_2 \end{cases} \quad (20)$$

If the reflectance spectrum R' at $(\Phi_{\text{inc}}^{pos2},\Phi_{\text{col}}^{pos2})$ is equal to R scaled by a factor s. Then the saturation S' is:

$$\begin{cases} S' = \lambda'_1 - \lambda'_2 \\ R'(\lambda'_1) = R'(\lambda'_2) = \frac{R'_{\text{max}}}{2} \\ \lambda'_1 > \lambda'_2 \end{cases} \quad (21)$$

where

$$\begin{cases} R'(\lambda'_1) = \frac{R(\lambda'_1)}{s} \\ R'(\lambda'_2) = \frac{R(\lambda'_2)}{s} \\ R'_{\text{max}} = \frac{R_{\text{max}}}{s} \end{cases} \quad (22)$$

From this, we find that:

$$\frac{R(\lambda'_2)}{s} = \frac{R(\lambda'_1)}{s} = \frac{R_{\text{max}}}{2s} \quad (23)$$

$$R(\lambda'_2) = R(\lambda'_1) = \frac{R_{\text{max}}}{2} \quad (24)$$

This means that $\lambda'_1 = \lambda_1$ and $\lambda'_2 = \lambda_2$. In other words, the full width at half max is stable by scaling, which results in the saturation S remaining constant along the $\Phi_{\text{inc}} + \Phi_{\text{col}} =$ cst axis (constant span).

5.3.2 Along the 'constant angle bisector' direction ($\Phi_{\text{inc}} - \Phi_{\text{col}} =$ cst)

Additionally, along the $\Phi_{\text{inc}} - \Phi_{\text{col}} =$ cst axis (constant angle bisector), brightness is constant and only hue changes. This means spectra are translations of one another. The full width at half max is also stable by translation so the saturation S remains constant along $\Phi_{\text{inc}} - \Phi_{\text{col}} =$ cst axis (constant angle bisector).

5.3.3 In the general case

All points in the $(\Phi_{\text{inc}},\Phi_{\text{col}})$ space can be reached by a combination of moves along the orthogonal 'constant span' ($\Phi_{\text{inc}} + \Phi_{\text{col}} =$ cst) and 'constant angle bisector' ($\Phi_{\text{inc}} - \Phi_{\text{col}} =$ cst) axes. We just showed the saturation S is constant along these two axes so it is actually constant in the whole $(\Phi_{\text{inc}},\Phi_{\text{col}})$ space.

6 Appendix 2: Comparison with other methods

6.1 Measurements at fixed angle configuration

The angle t between the multilayer structure and the normal to the surface of the feather (tilt) is highly variable between species of the same family ($sd = 19.36°$ in hummingbirds, as reported in table 2). This is in agreement with Osorio and Ham [15] who found tilt values t ranging from $-20°$ to $40°$. Even if the angle configuration $(\Phi_{\text{inc}}, \Phi_{\text{col}})$ is constant at the macroscopic scale, the configuration relative to the multilayer structure (θ_i, θ_r) may not be constant because of the variation in the tilt t between samples. This means measurements at fixed geometry cannot be compared between samples. For this reason, we warn against measurements of iridescent colours at a fixed angle, even when angular dependency is not studied.

6.2 Parameters estimation using constant illumination

Some goniometers only allow for the rotation of the collection fibre while the illumination fibre stays at a fixed position. Measurements realised with a such protocol can still be used with our method but this leads to a loss of statistical power.

If illumination is provided at a fixed angle $\Phi_{\text{inc}} = \alpha$:

$$\begin{aligned} B(\Phi_{\text{col}}) &= B_{\text{max}} \exp -\frac{\left(\frac{\alpha-\Phi_{\text{col}}}{2} - t\right)^2}{2\gamma_B^2} \\ &= B_{\text{max}} \exp -\frac{(\Phi_{\text{col}} + 2t - \alpha)^2}{8\gamma_B^2} \end{aligned} \tag{25}$$

So, $B(\Phi_{\text{col}})$ is still a normal function of Φ_{col} with the same maximum value B_{max} but with parameters $t^* = 2t - \alpha$ and $\gamma_B^* = 2\gamma_B$ for mean and standard deviation respectively.

Because the estimation of the parameters of a normal function through a regression is more reliable is the standard deviation is low, using anything else than a fixed normal as measurement line, such as a fixed illumination, to measure brightness parameters will result in a loss of statistical power.

Additionally, depending on the exact value of α, it may not be possible to have a fibre configuration where $\frac{\alpha+\Phi_{\text{col}}}{2} = t$ but the span between the fibres is still less than $90°$ (small angles assumption). In this case, data points never reach the maximum B_{max}, which makes parameters estimation very unreliable.

Finally, the new value of the mean t^* does not have a direct biological and physical interpretation, as opposed to t which is the tilt of the multilayer of thin-film structure.

For hue, if illumination is at fixed angle α:

$$H(\Phi_{\text{col}}) = H_{\text{max}} \cos(\gamma_H \frac{\alpha}{2} + \frac{\gamma_H}{2}\Phi_{\text{col}}) \tag{26}$$

The equation for hue at fixed illumination has a shape different from its general form depending on the span between the fibres, $\frac{\Phi_{\text{inc}}+\Phi_{\text{col}}}{2}$. There is a constant term in the cosine function and the new term for hue angular dependency is $\gamma_H^* = \frac{\gamma_H}{2}$. As we explain in the next section, the estimation of the parameters is more reliable for high values of γ_H. For this reason, the parameters estimation at fixed illumination may not be as precise as along the $\Phi_{\text{inc}} + \Phi_{\text{col}} = \text{cst}$ line.

6.3 Link with other variables of angular dependency for hue

6.3.1 Linear regression

Linear regression instead of cosine regression to estimate H_{max} and γ_H is common [15, 50–52]. Because the curvature of the cosine function in eq. (18), defining hue depending on the angular span, is often small, we obtain congruent results using either cosine or linear regression. However, this creates a systematic bias where H_{max} is more overestimated for samples with larger angle dependency γ_H. Indeed, a linear regression overestimates more the intercept value as the curvature of the function increases.

6.3.2 Difference between two angle configurations with the same angle bisector

The difference in hue between two angle configurations is sometimes used as a proxy for iridescence [53]. However, it is problematic because it leads to a very high correlation between hue and iridescence, as reported in Dakin and Montgomerie [18] ($R^2 > 0.95$).

We can prove mathematically this linear correlation. Let us focus on the difference between hue H_{pos1} at a given angle configuration $(\Phi^1_{\text{inc}}, \Phi^1_{\text{col}})$ and hue H_{max} at coincident geometry (i.e. $\Phi_{\text{inc}} + \Phi_{\text{col}} = \theta_i + \theta_r = 0$). It follows from eq. (18) that defines the hue at any angle configuration that:

$$H_{\text{pos1}} - H_{\text{max}} = H_{\text{max}} \left[\cos\left(\gamma_H \frac{\Phi^1_{\text{inc}} + \Phi^1_{\text{col}}}{2}\right) - 1\right] \tag{27}$$

From this equation, we see that if γ_H is constant or display low variability between samples, $H_{\text{pos1}} - H_{\text{max}}$ is proportional to H_{max}:

$$H_{\text{pos1}} - H_{\text{max}} \propto H_{\text{max}} \tag{28}$$

We can apply the same reasoning and prove the difference $H_{\text{pos2}} - H_{\text{max}}$ between hue H_{pos2} at $(\Phi^2_{\text{inc}}, \Phi^2_{\text{col}})$ and H_{max} is proportional to H_{max}:

$$H_{\text{pos2}} - H_{\text{max}} \propto H_{\text{max}} \tag{29}$$

Thus (doing eq. (28) – eq. (29)) the difference in hue between any two angle configurations $(\Phi^1_{\text{inc}}, \Phi^1_{\text{col}})$ and $(\Phi^2_{\text{inc}}, \Phi^2_{\text{col}})$ is proportional to H_{max}

$$H_{\text{pos1}} - H_{\text{pos2}} \propto H_{\text{max}} \tag{30}$$

This correlation between the two variables characterising hue in the angle space can lead to errors in

subsequent statistical inferences. On the opposite and we showed previously, the parameters proposed in this study (H_{max} and γ_H) do not have the same issue.

6.4 Link with other variables of angular dependency for brightness

We are providing the following comparison with variables that have previously used in the literature to describe brightness angular dependency. This means that values from previous studies using these variables can still be used in a meta-analysis or a discussion using our new variables B_{max}, t and γ_B. We however explain why they are less precise, less versatile and/or more time consuming than those measured under our unified framework.

6.4.1 FWHM and angular breadth

We have shown brightness is a Gaussian function of standard deviation γ_B along the line of 'constant span' ($\Phi_{\text{inc}} + \Phi_{\text{col}} = \text{cst}$ direction). Many studies previously characterised angular dependency in this direction using the full width at half max (hereafter FWHM) [11, 12, 15, 27, 54]. For a Gaussian function, there is an easy link between standard deviation and FWHM:

$$\begin{aligned} \text{FWHM} &= 2\gamma_B^* \sqrt{2 \ln 2} \\ &= 4\gamma_B \sqrt{2 \ln 2} \\ &\approx 4.71 \gamma_B \end{aligned} \tag{31}$$

Similarly, some studies use what they call angular breadth [38, 55–61], which they define as the range of angle where brightness is higher than 3 % of its maximum (threshold at 10 % for White et al. [60]):

$$\begin{aligned} \text{ang. breadth} &= 2\gamma_B^* \sqrt{4 \ln 10 - 2 \ln 3} \\ &= 4\gamma_B \sqrt{4 \ln 10 - 2 \ln 3} \\ &\approx 10.59 \gamma_B \end{aligned} \tag{32}$$

We see that these variables are proportional to γ_B in theory. However because they are computed from raw data, without any pre-processing or curve fitting, they are more sensitive to noise.

6.4.2 Hunter's specular gloss and integrating sphere

Multiple studies [52, 62, 63] use Hunter's gloss [64], defined by the ratio of specular to diffuse reflectance. This method is convenient because it can easily be achieved using an integrating sphere to capture the needed spectra in two measurements only (one at specular position without the sphere and one with the sphere to capture diffuse and specular reflectance).

This is equivalent of keeping the illumination at a fixed angle and measuring reflectance at all collection angles. We already know the brightness at the specular position is B_{max}. The diffuse reflection is the integral on all angle configurations of the brightness. Hence Hunter's specular gloss G using the notation defined in this study is :

$$G = \frac{B_{\text{max}}}{\iint B(\Phi_{\text{inc}}, \Phi_{\text{col}})\, d\Phi_{\text{inc}}\, d\Phi_{\text{col}}} \tag{33}$$

The integral of brightness for every angle configurations is $B_{\text{max}} \gamma_B^* \sqrt{2\pi}$ (integral of the normal function with maximum B_{max} and standard deviation γ_B^*), which gives:

$$G = \frac{1}{\gamma_B^* \sqrt{2\pi}} = \frac{1}{2\gamma_B \sqrt{2\pi}} \tag{34}$$

However, this is assuming the measurement of B_{max} was actually done at the normal to the multilayer $\frac{\Phi_{\text{inc}} + \Phi_{\text{col}}}{2} = t$. But there is no way to know whether it is the case without doing several goniometer measurements with different normal positions. Once this is done, γ_B can be estimated without doing additional integrating sphere measurements.

6.4.3 Difference/Quotient between max and another position with the same span

Some studies [38, 65, 66] use the difference or the quotient between the brightness at the fibre position where it is maximum and another position. With this approach, they find t and B_{max}.

The difference or the quotient between these two positions can easily be linked to γ_B because we know that $B(\Phi_{\text{inc}}, \Phi_{\text{col}})$ is a normal function of parameters t and γ_B.

However, this is very sensitive to noise and measurement error because B_{max} and t are estimated with only one data point and γ_B (or its equivalent variable) with only two data points.

7 Appendix 3: structural colours with pigmentary component

The framework we presented here focuses on purely structural iridescent colours. However many colours integrate both pigmentary and structural components [67, 68]. If there is a pigmentary component, it adds constant term B_{pigment} to brightness B:

$$B(\Phi_{\text{inc}}, \Phi_{\text{col}}) = B_{\text{irid}} + B_{\text{pigment}} \tag{35}$$

$$B(\Phi_{\text{inc}}, \Phi_{\text{col}}) = B_{\text{max}} \exp - \frac{\left(\frac{\Phi_{\text{inc}} - \Phi_{\text{col}}}{2} - t \right)^2}{2\gamma_B^2} + B_{\text{pigment}} \tag{36}$$

This can easily be investigated using our protocol and statistical framework. The only difference is that 4 parameters (B_{max}, t, γ_B and B_{pigment}) instead of 3 need to be estimated by running a non-linear regression on eq. (36) instead of eq. (8).

There are cases where the structural and pigmentary components of colour act on very different regions of the light spectrum. This happens for example in *Colias eurytheme* [69], where iridescence is restricted to the UV region while the visible region colour is caused by pigments. In this case, our method can be applied directly by restricting the studied wavelength range to the region of interest (this option is available in the code provided in ESM).

Number of measurements	Fibre configuration (number of studies)	Birds	Arthropods	Others
Single measurement	Single fixed angle (53)	[70–100]	[24, 31, 101–113]	Bony fishes [114]; Mammals [115]; Plants [28, 116–118]
	Single measurement relative to the structures orientation (6)	-	[34, 119–123]	-
Multiple measurements along a single line	Constant illumination (5)	[124]	[50, 69, 125]	Bacteria [126]
	Constant collection (2)	[18]	[9]	-
	Constant angle bisector (16)	[5, 48, 49, 52, 53, 127–132]	[12, 133–136]	-
	Constant span (16)	[7, 38, 61, 65]	[13, 55–59, 137–139]	Bony fishes [25]; Lizards [19, 140]
Multiple measurement lines	Multiple constant illuminations (4)	[141]	[11, 39]	Bacteria [142]
	Multiple constant collections (1)	[47]	-	
	Multiple constant spans (1)	[14]	-	
	Constant illumination & bisector (3)	-	[27, 143]	Bacteria [144]
	Multiple illumination & bisector (1)	-	[10]	-
	Constant illumination & span (3)	[15, 66]	[60]	-
	Constant span & bisector (6)	[4, 16, 54]	[20, 145, 146]	Gastropods [29]
	Constant illumination, span & bisector (4)	[51, 147]	[11, 148]	-

Table 3. Review of the methods used in the literature to study iridescent colours from multilayer or thin-films structure. The criteria we used for studies to be included in the table were the following (i) at least one quantitative reflectance measurement using a spectrometer (ii) functioning with white light (no monochromatic illumination) and (iii) the patch measured had to be described as iridescent in the article. A more detailed version of this table, with all angle configurations and colour variables used for each study is available in ESM. The terms 'constant illumination', 'constant collection', 'constant angle bisector' and 'constant span' are defined in fig. 3d.

References

[1] Maynard Smith, J and Harper, DA. Animal Signals. Reprint. Oxford series in ecology and evolution. OCLC: 553680850. Oxford: Oxford Univ. Press, 2009. 166 pp. ISBN: 978-0-19-852684-1 978-0-19-852685-8.

[2] Parker, AR. '515 Million Years of Structural Colour'. Journal of Optics A: Pure and Applied Optics 2.6 (2000), R15–R28. DOI: 10.1088/1464-4258/2/6/201.

[3] Doucet, SM and Meadows, MG. 'Iridescence: A Functional Perspective'. Journal of The Royal Society Interface 6 (Suppl 2 2009), S115–S132. DOI: 10.1098/rsif.2008.0395.focus. pmid: 19336344.

[4] Stavenga, DG, Leertouwer, HL, Marshall, NJ and Osorio, DC. 'Dramatic Colour Changes in a Bird of Paradise Caused by Uniquely Structured Breast Feather Barbules'. Proceedings of the Royal Society of London B: Biological Sciences 278.1715 (2011), pp. 2098–2104. DOI: 10.1098/rspb.2010.2293. pmid: 21159676.

[5] Wilts, BD, Michielsen, K, Raedt, HD and Stavenga, DG. 'Sparkling Feather Reflections of a Bird-of-Paradise Explained by Finite-Difference Time-Domain Modeling'. Proceedings of the National Academy of Sciences 111.12 (2014), pp. 4363–4368. DOI: 10.1073/pnas.1323611111. pmid: 24591592.

[6] Simpson, RK and McGraw, KJ. 'Two Ways to Display: Male Hummingbirds Show Different Color-Display Tactics Based on Sun Orientation'. Behavioral Ecology 29.3 (2018), pp. 637–648. DOI: 10.1093/beheco/ary016.

[7] Simpson, RK and McGraw, KJ. 'It's Not Just What You Have, but How You Use It: Solar-Positional and Behavioural Effects on Hummingbird Colour Appearance during Courtship'. Ecology Letters 0.0 (2018). DOI: 10.1111/ele.13125.

[8] Moyroud, E, Wenzel, T, Middleton, R, Rudall, PJ, Banks, H et al. 'Disorder in Convergent Floral Nanostructures Enhances Signalling to Bees'. Nature 550.7677 (2017), pp. 469–474. DOI: 10.1038/nature24285.

[9] Berthier, S, Charron, E and Boulenguez, J. 'Morphological Structure and Optical Properties of the Wings of Morphidae'. Insect Science 13.2 (2006), pp. 145–158. DOI: 10.1111/j.1744-7917.2006.00077.x.

[10] Edo, S, Okoshi, K, Kang, S, Tokita, M and Watanabe, J. 'Unique Reflection Property Due to Bumpy Multilayer Structure in Elytra of Rhomborrhina Unicolor'. Japanese Journal of Applied Physics 49 (4R 2010), p. 047201. DOI: 10.1143/JJAP.49.047201.

[11] Pirih, P, Wilts, BD and Stavenga, DG. 'Spatial Reflection Patterns of Iridescent Wings of Male Pierid Butterflies: Curved Scales Reflect at a Wider Angle than Flat Scales'. Journal of Comparative Physiology A 197.10 (2011), pp. 987–997. DOI: 10.1007/s00359-011-0661-6.

[12] Wickham, S, Large, MCJ, Poladian, L and Jermiin, LS. 'Exaggeration and Suppression of Iridescence: The Evolution of Two-Dimensional Butterfly Structural Colours'. Journal of The Royal Society Interface 3.6 (2006), pp. 99–109. DOI: 10.1098/rsif.2005.0071. pmid: 16849221.

[13] Parnell, AJ, Bradford, JE, Curran, EV, Washington, AL, Adams, G et al. 'Wing Scale Ultrastructure Underlying Convergent and Divergent Iridescent Colours in Mimetic Heliconius Butterflies'. Journal of The Royal Society Interface 15.141 (2018), p. 20170948. DOI: 10.1098/rsif.2017.0948. pmid: 29669892.

[14] Madsen, V, Dabelsteen, T, Osorio, D and Osorno, JL. 'Morphology and Ornamentation in Male Magnificent Frigatebirds: Variation with Age Class and Mating Status'. The American Naturalist 169.S1 (2007), S93–S111. DOI: 10.1086/510096.

[15] Osorio, DC and Ham, AD. 'Spectral Reflectance and Directional Properties of Structural Coloration in Bird Plumage'. Journal of Experimental Biology 205.14 (2002), pp. 2017–2027. pmid: 12089207.

[16] Meadows, MG, Morehouse, NI, Rutowski, RL, Douglas, JM and McGraw, KJ. 'Quantifying Iridescent Coloration in Animals: A Method for Improving Repeatability'. Behavioral Ecology and Sociobiology 65.6 (2011), pp. 1317–1327. DOI: 10.1007/s00265-010-1135-5. pmid: 876.

[17] Montgomerie, R. 'Analyzing Colors'. In: Bird Coloration, Volume 1: Mechanisms and Measurements. Ed. by Hill, GE and McGraw, KJ. Vol. 1. 2 vols. Bird Coloration. Harvard University Press, 2006, p. 640. ISBN: 978-0-674-01893-8.

[18] Dakin, R and Montgomerie, R. 'Eye for an Eyespot: How Iridescent Plumage Ocelli Influence Peacock Mating Success'. Behavioral Ecology 24.5 (2013), pp. 1048–1057. DOI: 10.1093/beheco/art045.

[19] Pérez i de Lanuza, G and Font, E. 'Now You See Me, Now You Don't: Iridescence Increases the Efficacy of Lizard Chromatic Signals'. Naturwissenschaften 101.10 (2014), pp. 831–837. DOI: 10.1007/s00114-014-1224-9.

[20] Waldron, SJ, Endler, JA, Valkonen, JK, Honma, A, Dobler, S et al. 'Experimental Evidence Suggests That Specular Reflectance and Glossy Appearance Help Amplify Warning Signals'. Scientific Reports 7.1 (2017), p. 257. DOI: 10.1038/s41598-017-00217-5.

[21] Gur, D, Palmer, BA, Leshem, B, Oron, D, Fratzl, P et al. 'The Mechanism of Color Change in the Neon Tetra Fish: A Light-Induced Tunable Photonic Crystal Array'. Angewandte Chemie International Edition 54.42 (2015), pp. 12426–12430. DOI: 10.1002/anie.201502268.

[22] Land, MF. 'A Multilayer Interference Reflector in the Eye of the Scallop, Pecten Maximus'. Journal of Experimental Biology 45.3 (1966), pp. 433–447.

[23] Brink, DJ and Lee, ME. 'Thin-Film Biological Reflectors: Optical Characterization of the Chrysiridia Croesus Moth'. Applied Optics 37.19 (1998), pp. 4213–4217. DOI: 10.1364/AO.37.004213.

[24] Chae, J and Nishida, S. 'Spectral Patterns of the Iridescence in the Males of Sapphirina (Copepoda: Poecilostomatoida)'. Journal of the Marine Biological Association of the United Kingdom 79.3 (1999), pp. 437–443. DOI: 10.1017/S0025315498000563.

[25] Mäthger, LM, Land, MF, Siebeck, UE and Marshall, NJ. 'Rapid Colour Changes in Multilayer Reflecting Stripes in the Paradise Whiptail, Pentapodus Paradiseus'. Journal of Experimental Biology 206.20 (2003), pp. 3607–3613. DOI: 10.1242/jeb.00599. pmid: 12966052.

[26] Kinoshita, S and Yoshioka, S. 'Structural Colors in Nature: The Role of Regularity and Irregularity in the Structure'. ChemPhysChem 6.8 (2005), pp. 1442–1459. DOI: 10.1002/cphc.200500007.

[27] Stavenga, DG, Wilts, BD, Leertouwer, HL and Hariyama, T. 'Polarized Iridescence of the Multilayered Elytra of the Japanese Jewel Beetle, Chrysochroa Fulgidissima'. Philosophical Transactions of the Royal Society B: Biological Sciences 366.1565 (2011), pp. 709–723. DOI: 10.1098/rstb.2010.0197. pmid: 21282175.

[28] Chandler, CJ, Wilts, BD, Vignolini, S, Brodie, J, Steiner, U et al. 'Structural Colour in Chondrus Crispus'. Scientific Reports 5 (2015), p. 11645. DOI: 10.1038/srep11645.

[29] Brink, DJ, Berg, NG van der and Botha, AJ. 'Iridescent Colors on Seashells: An Optical and Structural Investigation of Helcion Pruinosus'. Applied Optics 41.4 (2002), pp. 717–722. DOI: 10.1364/AO.41.000717.

[30] Land, MF. 'The Physics and Biology of Animal Reflectors'. Progress in Biophysics and Molecular Biology 24 (1972), pp. 75–106. DOI: 10.1016/0079-6107(72)90004-1. pmid: 4581858.

[31] Schultz, TD and Rankin, MA. 'The Ultrastructure of the Epicuticular Interference Reflectors of Tiger Beetles (Cicindela)'. Journal of Experimental Biology 117.1 (1985), pp. 87–110.

[32] Parker, AR, McKenzie, DR and Large, MCJ. 'Multilayer Reflectors in Animals Using Green and Gold Beetles as Contrasting Examples'. Journal of Experimental Biology 201.9 (1998), pp. 1307–1313. pmid: 9547312.

[33] Kinoshita, S, Yoshioka, S and Miyazaki, J. 'Physics of Structural Colors'. Reports on Progress in Physics 71.7 (2008), p. 076401. DOI: 10.1088/0034-4885/71/7/076401.

[34] Huxley, J. 'The Basis of Structural Colour Variation in Two Species of Papilio'. Journal of Entomology Series A, General Entomology 50.1 (1975), pp. 9–22. DOI: 10.1111/j.1365-3032.1975.tb00087.x.

[35] Vukusic, P, Sambles, JR, Lawrence, CR and Wootton, RJ. 'Limited-View Iridescence in the Butterfly Ancyluris Meliboeus'. Proceedings of the Royal Society of London B: Biological Sciences 269.1486 (2002), pp. 7–14. DOI: 10.1098/rspb.2001.1836. pmid: 11788030.

[36] Del Hoyo, J, Elliott, A, Sargatal, J, Christie, DA and de Juana, E. Handbook of the Birds of the World Alive. 2017. URL: hbw.com.

[37] McGuire, JA, Witt, CC, Remsen, JVJ, Corl, A, Rabosky, DL et al. 'Molecular Phylogenetics and the Diversification of Hummingbirds'. Current Biology 24.8 (2014), pp. 910–916. DOI: 10.1016/j.cub.2014.03.016. pmid: 24704078.

[38] Van Wijk, S, Bélisle, M, Garant, D and Pelletier, F. 'A Reliable Technique to Quantify the Individual Variability of Iridescent Coloration in Birds'. Journal of Avian Biology 47.2 (2016), pp. 227–234. DOI: 10.1111/jav.00750.

[39] Plattner, L. 'Optical Properties of the Scales of Morpho Rhetenor Butterflies: Theoretical and Experimental Investigation of the Back-Scattering of Light in the Visible Spectrum'. Journal of The Royal Society Interface 1.1 (2004), pp. 49–59. DOI: 10.1098/rsif.2004.0006. pmid: 16849152.

[40] Berthier, S. Iridescences: The Physical Colors of Insects. New York: Springer-Verlag, 2007. ISBN: 978-0-387-34119-4.

[41] Chen, DM and Goldsmith, TH. 'Four Spectral Classes of Cone in the Retinas of Birds'. Journal of Comparative Physiology A 159.4 (1986), pp. 473–479. DOI: 10.1007/BF00604167.

[42] Maia, R, Eliason, CM, Bitton, PP, Doucet, SM and Shawkey, MD. 'Pavo: An R Package for the Analysis, Visualization and Organization of Spectral Data'. Methods in Ecology and Evolution 4.10 (2013), pp. 906–913. DOI: 10.1111/2041-210X.12069.

[43] Nakagawa, S and Schielzeth, H. 'Repeatability for Gaussian and Non-Gaussian Data: A Practical Guide for Biologists'. Biological Reviews 85.4 (2010), pp. 935–956. DOI: 10.1111/j.1469-185X.2010.00141.x. pmid: 20569253.

[44] Evans, SR, Hinks, AE, Wilkin, TA and Sheldon, BC. 'Age, Sex and Beauty: Methodological Dependence of Age- and Sex-Dichromatism in the Great Tit Parus Major'. Biological Journal of the Linnean Society 101.4 (2010), pp. 777–796. DOI: 10.1111/j.1095-8312.2010.01548.x.

[45] Midamegbe, A, Grégoire, A, Staszewski, V, Perret, P, Lambrechts, MM et al. 'Female Blue Tits with Brighter Yellow Chests Transfer More Carotenoids to Their Eggs after an Immune Challenge'. Oecologia 173.2 (2013), pp. 387–397. DOI: 10.1007/s00442-013-2617-8.

[46] Charmantier, A, Wolak, ME, Grégoire, A, Fargevieille, A and Doutrelant, C. 'Colour Ornamentation in the Blue Tit: Quantitative Genetic (Co)Variances across Sexes'. Heredity 118.2 (2017), pp. 125–134. DOI: 10.1038/hdy.2016.70.

[47] Eliason, CM and Shawkey, MD. 'A Photonic Heterostructure Produces Diverse Iridescent Colours in Duck Wing Patches'. Journal of The Royal Society Interface 9.74 (2012), pp. 2279–2289. DOI: 10.1098/rsif.2012.0118. pmid: 22491981.

[48] Stavenga, DG, Leertouwer, HL and Wilts, BD. 'Magnificent Magpie Colours by Feathers with Layers of Hollow Melanosomes'. Journal of Experimental Biology 221.4 (2018), jeb174656. DOI: 10.1242/jeb.174656. pmid: 29361607.

[49] Stavenga, DG, van der Kooi, CJ and Wilts, BD. 'Structural Coloured Feathers of Mallards Act by Simple Multilayer Photonics'. Journal of The Royal Society Interface 14.133 (2017), p. 20170407. DOI: 10.1098/rsif.2017.0407. pmid: 28768883.

[50] Rutowski, RL, Macedonia, JM, Kemp, DJ and Taylor-Taft, L. 'Diversity in Structural Ultraviolet Coloration among Female Sulphur Butterflies (Coliadinae, Pieridae)'. Arthropod Structure & Development 36.3 (2007), pp. 280–290. DOI: 10.1016/j.asd.2006.11.005.

[51] Eliason, CM, Bitton, PP and Shawkey, MD. 'How Hollow Melanosomes Affect Iridescent Colour Production in Birds'. Proc. R. Soc. B 280.1767 (2013), p. 20131505. DOI: 10.1098/rspb.2013.1505. pmid: 23902909.

[52] Igic, B, Fecheyr-Lippens, D, Xiao, M, Chan, A, Hanley, D et al. 'A Nanostructural Basis for Gloss of Avian Eggshells'. Journal of The Royal Society Interface 12.103 (2015), p. 20141210. DOI: 10.1098/rsif.2014.1210. pmid: 25505139.

[53] Maia, R, Caetano, JVO, Báo, SN and Macedo, RH. 'Iridescent Structural Colour Production in Male Blue-Black Grassquit Feather Barbules: The Role of Keratin and Melanin'. Journal of The Royal Society Interface 6 (Suppl 2 2009), S203–S211. DOI: 10.1098/rsif.2008.0460.focus. pmid: 19141431.

[54] Brink, DJ and van der Berg, NG. 'Structural Colours from the Feathers of the Bird Bostrychia Hagedash'. Journal of Physics D: Applied Physics 37.5 (2004), p. 813. DOI: 10.1088/0022-3727/37/5/025.

[55] Kemp, DJ, Vukusic, P and Rutowski, RL. 'Stress□mediated Covariance between Nano□structural Architecture and Ultraviolet Butterfly Coloration'. Functional Ecology 20.2 (2006), pp. 282–289. DOI: 10.1111/j.1365-2435.2006.01100.x.

[56] Rutowski, RL, Macedonia, JM, Merry, JW, Morehouse, NI, Yturralde, K et al. 'Iridescent Ultraviolet Signal in the Orange Sulphur Butterfly (Colias Eurytheme): Spatial, Temporal and Spectral Properties'. Biological Journal of the Linnean Society 90.2 (2007), pp. 349–364. DOI: 10.1111/j.1095-8312.2007.00749.x.

[57] Kemp, DJ and Rutowski, RL. 'Condition Dependence, Quantitative Genetics, and the Potential Signal Content of Iridescent Ultraviolet Butterfly Coloration'. Evolution 61.1 (2007), pp. 168–183. DOI: 10.1111/j.1558-5646.2007.00014.x.

[58] Kemp, DJ, Macedonia, JM, Ball, TS and Rutowski, RL. 'Potential Direct Fitness Consequences of Ornament-Based Mate Choice in a Butterfly'. Behavioral Ecology and Sociobiology 62.6 (2008), pp. 1017–1026. DOI: 10.1007/s00265-007-0529-5.

[59] Kemp, DJ. 'Female Mating Biases for Bright Ultraviolet Iridescence in the Butterfly Eurema Hecabe (Pieridae)'. Behavioral Ecology 19.1 (2008), pp. 1–8. DOI: 10.1093/beheco/arm094.

[60] White, TE, Zeil, J and Kemp, DJ. 'Signal Design and Courtship Presentation Coincide for Highly Biased Delivery of an Iridescent Butterfly Mating Signal'. Evolution 69.1 (2015), pp. 14–25. DOI: 10.1111/evo.12551.

[61] Van Wijk, S, Bourret, A, Bélisle, M, Garant, D and Pelletier, F. 'The Influence of Iridescent Coloration Directionality on Male Tree Swallows' Reproductive Success at Different Breeding Densities'. Behavioral Ecology and Sociobiology 70.9 (2016), pp. 1557–1569. DOI: 10.1007/s00265-016-2164-5.

[62] Maia, R, D'Alba, L and Shawkey, MD. 'What Makes a Feather Shine? A Nanostructural Basis for Glossy Black Colours in Feathers'. Proceedings of the Royal Society of London B: Biological Sciences 278.1714 (2011), pp. 1973–1980. DOI: 10.1098/rspb.2010.1637. pmid: 21123257.

[63] Iskandar, JP, Eliason, CM, Astrop, T, Igic, B, Maia, R et al. 'Morphological Basis of Glossy Red Plumage Colours'. Biological Journal of the Linnean Society 119.2 (2016), pp. 477–487. DOI: 10.1111/bij.12810.

[64] Hunter, RS. 'Methods of Determining Gloss'. Journal of Research of the National Bureau of Standards 18 (1937), p. 23. DOI: 10.6028/jres.018.006.

[65] Meadows, MG, Roudybush, TE and McGraw, KJ. 'Dietary Protein Level Affects Iridescent Coloration in Anna's Hummingbirds, Calypte Anna'. Journal of Experimental Biology 215.16 (2012), pp. 2742–2750. DOI: 10.1242/jeb.069351. pmid: 22837446.

[66] Loyau, A, Gomez, D, Moureau, B, Théry, M, Hart, NS et al. 'Iridescent Structurally Based Coloration of Eyespots Correlates with Mating Success in the Peacock'. Behavioral Ecology 18.6 (2007), pp. 1123–1131. DOI: 10.1093/beheco/arm088.

[67] Prum, RO. 'Anatomy, Physics, and Evolution of Structural Colors'. In: Bird Coloration, Volume 1: Mechanisms and Measurements. Ed. by Hill, GE and McGraw, KJ. Vol. 1. 2 vols. Bird Coloration. Harvard University Press, 2006, p. 640. ISBN: 978-0-674-01893-8.

[68] D'Alba, L, Kieffer, L and Shawkey, MD. 'Relative Contributions of Pigments and Biophotonic Nanostructures to Natural Color Production: A Case Study in Budgerigar (Melopsittacus Undulatus) Feathers'. Journal of Experimental Biology 215.8 (2012), pp. 1272–1277. DOI: 10.1242/jeb.064907. pmid: 22442364.

[69] Rutowski, RL, Macedonia, JM, Morehouse, NI and Taylor-Taft, L. 'Pterin Pigments Amplify Iridescent Ultraviolet Signal in Males of the Orange Sulphur Butterfly, Colias Eurytheme'. Proceedings of the Royal Society of London B: Biological Sciences 272.1578 (2005), pp. 2329–2335. DOI: 10.1098/rspb.2005.3216. pmid: 16191648.

[70] Bennett, ATD, Cuthill, IC, Partridge, JC and Lunau, K. 'Ultraviolet Plumage Colors Predict Mate Preferences in Starlings'. Proceedings of the National Academy of Sciences 94.16 (1997), pp. 8618–8621. DOI: 10.1073/pnas.94.16.8618. pmid: 9238026.

[71] Perrier, C, de Lope, F, Møller, AP and Ninni, P. 'Structural Coloration and Sexual Selection in the Barn Swallow Hirundo Rustica'. Behavioral Ecology 13.6 (2002), pp. 728–736. DOI: 10.1093/beheco/13.6.728.

[72] Doucet, SM and Montgomerie, R. 'Multiple Sexual Ornaments in Satin Bowerbirds: Ultraviolet Plumage and Bowers Signal Different Aspects of Male Quality'. Behavioral Ecology 14.4 (2003), pp. 503–509. DOI: 10.1093/beheco/arg035.

[73] Doucet, SM and Montgomerie, R. 'Structural Plumage Colour and Parasites in Satin Bowerbirds Ptilonorhynchus Violaceus: Implications for Sexual Selection'. Journal of Avian Biology 34.3 (2003), pp. 237–242. DOI: 10.1034/j.1600-048X.2003.03113.x.

[74] Zi, J, Yu, X, Li, Y, Hu, X, Xu, C et al. 'Coloration Strategies in Peacock Feathers'. Proceedings of the National Academy of Sciences 100.22 (2003), pp. 12576–12578. DOI: 10.1073/pnas.2133313100. pmid: 14557541.

[75] McGraw, KJ. 'Multiple UV Reflectance Peaks in the Iridescent Neck Feathers of Pigeons'. Naturwissenschaften 91.3 (2004), pp. 125–129. DOI: 10.1007/s00114-003-0498-0.

[76] Costa, FJV and Macedo, RH. 'Coccidian Oocyst Parasitism in the Blue-Black Grassquit: Influence on Secondary Sex Ornaments and Body Condition'. Animal Behaviour 70.6 (2005), pp. 1401–1409. DOI: 10.1016/j.anbehav.2005.03.024.

[77] Hill, GE, Doucet, SM and Buchholz, R. 'The Effect of Coccidial Infection on Iridescent Plumage Coloration in Wild Turkeys'. Animal Behaviour 69.2 (2005), pp. 387–394. DOI: 10.1016/j.anbehav.2004.03.013.

[78] Komdeur, J, Oorebeek, M, van Overveld, T and Cuthill, IC. 'Mutual Ornamentation, Age, and Reproductive Performance in the European Starling'. Behavioral Ecology 16.4 (2005), pp. 805–817. DOI: 10.1093/beheco/ari059.

[79] Shawkey, MD, Hauber, ME, Estep, LK and Hill, GE. 'Evolutionary Transitions and Mechanisms of Matte and Iridescent Plumage Coloration in Grackles and Allies (Icteridae)'. Journal of The Royal Society Interface 3.11 (2006), pp. 777–786. DOI: 10.1098/rsif.2006.0131. pmid: 17015306.

[80] Bitton, PP, O'Brien, EL and Dawson, RD. 'Plumage Brightness and Age Predict Extrapair Fertilization Success of Male Tree Swallows, Tachycineta Bicolor'. Animal Behaviour 74.6 (2007), pp. 1777–1784. DOI: 10.1016/j.anbehav.2007.03.018.

[81] Bitton, PP and Dawson, RD. 'Age-Related Differences in Plumage Characteristics of Male Tree Swallows Tachycineta Bicolor : Hue and Brightness Signal Different Aspects of Individual Quality'. Journal of Avian Biology 39.4 (2008), pp. 446–452. DOI: 10.1111/j.0908-8857.2008.04283.x.

[82] Bitton, PP, Dawson, RD and Ochs, CL. 'Plumage Characteristics, Reproductive Investment and Assortative Mating in Tree Swallows Tachycineta Bicolor'. Behavioral Ecology and Sociobiology 62.10 (2008), pp. 1543–1550. DOI: 10.1007/s00265-008-0583-7.

[83] Galván, I and Møller, AP. 'Different Roles of Natural and Sexual Selection on Senescence of Plumage Colour in the Barn Swallow'. Functional Ecology 23.2 (2009), pp. 302–309. DOI: 10.1111/j.1365-2435.2008.01504.x.

[84] Eliason, CM and Shawkey, MD. 'Rapid, Reversible Response of Iridescent Feather Color to Ambient Humidity'. Optics Express 18.20 (2010), pp. 21284–21292. DOI: 10.1364/OE.18.021284.

[85] Legagneux, P, Théry, M, Guillemain, M, Gomez, D and Bretagnolle, V. 'Condition Dependence of Iridescent Wing Flash-Marks in Two Species of Dabbling Ducks'. Behavioural Processes 83.3 (2010), pp. 324–330. DOI: 10.1016/j.beproc.2010.01.017.

[86] Maia, R and Macedo, RH. 'Achieving Luster: Prenuptial Molt Pattern Predicts Iridescent Structural Coloration in Blue-Black Grassquits'. Journal of Ornithology 152.2 (2011), pp. 243–252. DOI: 10.1007/s10336-010-0576-y.

[87] Savard, JF, Keagy, J and Borgia, G. 'Blue, Not UV, Plumage Color Is Important in Satin Bowerbird Ptilonorhynchus Violaceus Display'. Journal of Avian Biology 42.1 (2011), pp. 80–84. DOI: 10.1111/j.1600-048X.2010.05128.x.

[88] Eliason, CM and Shawkey, MD. 'Decreased Hydrophobicity of Iridescent Feathers: A Potential Cost of Shiny Plumage'. The Journal of Experimental Biology 214 (Pt 13 2011), pp. 2157–2163. DOI: 10.1242/jeb.055822. pmid: 21653809.

[89] Lee, E, Miyazaki, J, Yoshioka, S, Lee, H and Sugita, S. 'The Weak Iridescent Feather Color in the Jungle Crow Corvus Macrorhynchos'. Ornithological Science 11.1 (2012), pp. 59–64. DOI: 10.2326/osj.11.59.

[90] Legagneux, P, Clark, RG, Guillemain, M, Eraud, C, Théry, M et al. 'Large-Scale Geographic Variation in Iridescent Structural Ornaments of a Long-Distance Migratory Bird'. Journal of Avian Biology 43.4 (2012), pp. 355–361. DOI: 10.1111/j.1600-048X.2012.05666.x.

[91] Maia, R, Rubenstein, DR and Shawkey, MD. 'Key Ornamental Innovations Facilitate Diversification in an Avian Radiation'. Proceedings of the National Academy of Sciences 110.26 (2013), pp. 10687–10692. DOI: 10.1073/pnas.1220784110. pmid: 23754395.

[92] Leclaire, S, Pierret, P, Chatelain, M and Gasparini, J. 'Feather Bacterial Load Affects Plumage Condition, Iridescent Color, and Investment in Preening in Pigeons'. Behavioral Ecology 25.5 (2014), pp. 1192–1198. DOI: 10.1093/beheco/aru109.

[93] Eliason, CM, Maia, R and Shawkey, MD. 'Modular Color Evolution Facilitated by a Complex Nanostructure in Birds'. Evolution 69.2 (2015), pp. 357–367. DOI: 10.1111/evo.12575.

[94] Lee, CC, Liao, SF and Vukusic, P. 'Measuring and Modelling the Reflectance Spectra of Male Swinhoe's Pheasant Feather Barbules'. Journal of The Royal Society Interface 12.105 (2015), p. 20141354. DOI: 10.1098/rsif.2014.1354. pmid: 25788537.

[95] Mahapatra, BB, Marathe, SA, Meyer-Rochow, VB and Mishra, M. 'A Closer Look at the Feather Coloration in the Male Purple Sunbird, Nectarinia Asiatica'. Micron 85 (2016), pp. 44–50. DOI: 10.1016/j.micron.2016.04.001.

[96] Maia, R, Rubenstein, DR and Shawkey, MD. 'Selection, Constraint, and the Evolution of Coloration in African Starlings'. Evolution 70.5 (2016), pp. 1064–1079. DOI: 10.1111/evo.12912.

[97] Nam, HY, Lee, SI, Lee, J, Choi, CY and Choe, JC. 'Multiple Structural Colors of the Plumage Reflect Age, Sex, and Territory Ownership in the Eurasian Magpie Pica Pica'. Acta Ornithologica 51.1 (2016), pp. 83–92. DOI: 10.3161/00016454AO2016.51.1.007.

[98] Ornelas, JF, González, C, Hernández-Baños, BE and García-Moreno, J. 'Molecular and Iridescent Feather Reflectance Data Reveal Recent Genetic Diversification and Phenotypic Differentiation in a Cloud Forest Hummingbird'. Ecology and Evolution 6.4 (2016), pp. 1104–1127. DOI: 10.1002/ece3.1950.

[99] Vaquero-Alba, I, McGowan, A, Pincheira-Donoso, D, Evans, MR and Dall, SRX. 'A Quantitative Analysis of Objective Feather Color Assessment: Measurements in the Laboratory Do Not Reflect True Plumage Color'. The Auk 133.3 (2016), pp. 325–337. DOI: 10.1642/AUK-16-19.1.

[100] Quinard, A, Cézilly, F, Motreuil, S, Rossi, JM and Biard, C. 'Reduced Sexual Dichromatism, Mutual Ornamentation, and Individual Quality in the Monogamous Zenaida Dove Zenaida Aurita'. Journal of Avian Biology 48.4 (2017), pp. 489–501. DOI: 10.1111/jav.00902.

[101] Mossakowski, D. 'Reflection Measurements Used in the Analysis of Structural Colours of Beetles'. Journal of Microscopy 116.3 (1979), pp. 351–364. DOI: 10.1111/j.1365-2818.1979.tb00220.x.

[102] Tada, H, Mann, SE, Miaoulis, IN and Wong, PY. 'Effects of a Butterfly Scale Microstructure on the Iridescent Color Observed at Different Angles'. Optics Express 5.4 (1999), pp. 87–92. DOI: 10.1364/OE.5.000087.

[103] Vukusic, P, Sambles, R, Lawrence, C and Wakely, G. 'Sculpted-Multilayer Optical Effects in Two Species of Papilio Butterfly'. Applied Optics 40.7 (2001), pp. 1116–1125. DOI: 10.1364/AO.40.001116.

[104] Hariyama, T, Takaku, Y, Hironaka, M, Horiguchi, H, Komiya, Y et al. 'The Origin of the Iridescent Colors in Coleopteran Elytron'. Forma 17.2 (2002), pp. 123–132.

[105] Kurachi, M, Takaku, Y, Komiya, Y and Hariyama, T. 'The Origin of Extensive Colour Polymorphism in Plateumaris Sericea (Chrysomelidae, Coleoptera)'. Naturwissenschaften 89.7 (2002), pp. 295–298. DOI: 10.1007/s00114-002-0332-0.

[106] Liu, F, Dong, BQ, Liu, XH, Zheng, YM and Zi, J. 'Structural Color Change in Longhorn Beetles Tmesisternus Isabellae'. Optics Express 17.18 (2009), pp. 16183–16191. DOI: 10.1364/OE.17.016183.

[107] Schultz, TD and Fincke, OM. 'Structural Colours Create a Flashing Cue for Sexual Recognition and Male Quality in a Neotropical Giant Damselfly'. Functional Ecology 23.4 (2009), pp. 724–732. DOI: 10.1111/j.1365-2435.2009.01584.x.

[108] Ingram, AL, Deparis, O, Boulenguez, J, Kennaway, G, Berthier, S et al. 'Structural Origin of the Green Iridescence on the Chelicerae of the Red-Backed Jumping Spider, Phidippus Johnsoni (Salticidae: Araneae)'. Arthropod Structure & Development 40.1 (2011), pp. 21–25. DOI: 10.1016/j.asd.2010.07.006.

[109] Kuitunen, K and Gorb, SN. 'Effects of Cuticle Structure and Crystalline Wax Coverage on the Coloration in Young and Old Males of Calopteryx Splendens and Calopteryx Virgo'. Zoology 114.3 (2011), pp. 129–139. DOI: 10.1016/j.zool.2011.01.003.

[110] Gur, D, Leshem, B, Farstey, V, Oron, D, Addadi, L et al. 'Light-Induced Color Change in the Sapphirinid Copepods: Tunable Photonic Crystals'. Advanced Functional Materials 26.9 (2016), pp. 1393–1399. DOI: 10.1002/adfm.201504339.

[111] Wilts, BD, Giraldo, MA and Stavenga, DG. 'Unique Wing Scale Photonics of Male Rajah Brooke's Birdwing Butterflies'. Frontiers in Zoology 13 (2016), p. 36. DOI: 10.1186/s12983-016-0168-7.

[112] Onelli, OD, Kamp, T van de, Skepper, JN, Powell, J, Rolo, TdS et al. 'Development of Structural Colour in Leaf Beetles'. Scientific Reports 7.1 (2017), p. 1373. DOI: 10.1038/s41598-017-01496-8.

[113] Trzeciak, TM, Wilts, BD, Stavenga, DG and Vukusic, P. 'Variable Multilayer Reflection Together with Long-Pass Filtering Pigment Determines the Wing Coloration of Papilionid Butterflies of the Nireus Group'. Optics Express 20.8 (2012), pp. 8877–8890. DOI: 10.1364/OE.20.008877.

[114] Gur, D, Leshem, B, Oron, D, Weiner, S and Addadi, L. 'The Structural Basis for Enhanced Silver Reflectance in Koi Fish Scale and Skin'. Journal of the American Chemical Society 136.49 (2014), pp. 17236–17242. DOI: 10.1021/ja509340c.

[115] Snyder, HK, Maia, R, D'Alba, L, Shultz, AJ, Rowe, KMC et al. 'Iridescent Colour Production in Hairs of Blind Golden Moles (Chrysochloridae)'. Biology Letters 8.3 (2012), pp. 393–396. DOI: 10.1098/rsbl.2011.1168. pmid: 22279154.

[116] Lee, DW. 'Ultrastructural Basis and Function of Iridescent Blue Colour of Fruits in Elaeocarpus'. Nature 349.6306 (1991), pp. 260–262. DOI: 10.1038/349260a0.

[117] Lee, DW, Taylor, GT and Irvine, AK. 'Structural Fruit Coloration in Delarbrea Michieana (Araliaceae)'. International Journal of Plant Sciences 161.2 (2000), pp. 297–300. DOI: 10.1086/314249.

[118] Vignolini, S, Rudall, PJ, Rowland, AV, Reed, A, Moyroud, E et al. 'Pointillist Structural Color in Pollia Fruit'. Proceedings of the National Academy of Sciences 109.39 (2012), pp. 15712–15715. DOI: 10.1073/pnas.1210105109. pmid: 23019355.

[119] Kemp, DJ. 'Heightened Phenotypic Variation and Age-Based Fading of Ultraviolet Butterfly Wing Coloration'. Evolutionary Ecology Research 8.3 (2006), pp. 515–527.

[120] Papke, RS, Kemp, DJ and Rutowski, RL. 'Multimodal Signalling: Structural Ultraviolet Reflectance Predicts Male Mating Success Better than Pheromones in the Butterfly Colias Eurytheme L. (Pieridae)'. Animal Behaviour 73.1 (2007), pp. 47–54. DOI: 10.1016/j.anbehav.2006.07.004.

[121] Pegram, KV, Nahm, AC, Rutowski, RL and Todd, S. 'Warning Color Changes in Response to Food Deprivation in the Pipevine Swallowtail Butterfly, Battus Philenor'. Journal of Insect Science 13.1 (2013). DOI: 10.1673/031.013.11001.

[122] Kemp, DJ, Jones, D, Macedonia, JM and Krockenberger, AK. 'Female Mating Preferences and Male Signal Variation in Iridescent Hypolimnas Butterflies'. Animal Behaviour 87 (2014), pp. 221–229. DOI: 10.1016/j.anbehav.2013.11.001.

[123] Thurman, TJ and Seymoure, BM. 'A Bird's Eye View of Two Mimetic Tropical Butterflies: Coloration Matches Predator's Sensitivity'. Journal of Zoology 298.3 (2016), pp. 159–168. DOI: 10.1111/jzo.12305.

[124] Parra, JL. 'Color Evolution in the Hummingbird Genus Coeligena'. Evolution 64.2 (2010), pp. 324–335. DOI: 10.1111/j.1558-5646.2009.00827.x. pmid: 19703221.

[125] Imafuku, M and Ogihara, N. 'Wing Scale Orientation Alters Reflection Directions in the Green Hairstreak Chrysozephyrus Smaragdinus (Lycaenidae; Lepidoptera)'. Zoological Science 33.6 (2016), pp. 616–622. DOI: 10.2108/zs160041.

[126] Kientz, B, Ducret, A, Luke, S, Vukusic, P, Mignot, T et al. 'Glitter-like Iridescence within the Bacteroidetes Especially Cellulophaga Spp.: Optical Properties and Correlation with Gliding Motility'. PLOS ONE 7.12 (2012), e52900. DOI: 10.1371/journal.pone.0052900.

[127] Doucet, SM, Shawkey, MD, Hill, GE and Montgomerie, R. 'Iridescent Plumage in Satin Bowerbirds: Structure, Mechanisms and Nanostructural Predictors of Individual Variation in Colour'. Journal of Experimental Biology 209.2 (2006), pp. 380–390. DOI: 10.1242/jeb.01988. pmid: 16391360.

[128] Yin, H, Shi, L, Sha, J, Li, Y, Qin, Y et al. 'Iridescence in the Neck Feathers of Domestic Pigeons'. Physical Review E 74.5 (2006), p. 051916. DOI: 10.1103/PhysRevE.74.051916.

[129] Yoshioka, S, Nakamura, E and Kinoshita, S. 'Origin of Two-Color Iridescence in Rock Dove's Feather'. Journal of the Physical Society of Japan 76.1 (2007), p. 013801. DOI: 10.1143/JPSJ.76.013801.

[130] Shawkey, MD, D'Alba, L, Wozny, J, Eliason, C, Koop, JAH et al. 'Structural Color Change Following Hydration and Dehydration of Iridescent Mourning Dove (Zenaida Macroura) Feathers'. Zoology 114.2 (2011), pp. 59–68. DOI: 10.1016/j.zool.2010.11.001.

[131] Yoshioka, S and Kinoshita, S. 'Direct Determination of the Refractive Index of Natural Multilayer Systems'. Physical Review E 83.5 (2011), p. 051917. DOI: 10.1103/PhysRevE.83.051917.

[132] Stavenga, DG, Leertouwer, HL, Osorio, DC and Wilts, BD. 'High Refractive Index of Melanin in Shiny Occipital Feathers of a Bird of Paradise'. Light: Science & Applications 4.1 (2015), e243. DOI: 10.1038/lsa.2015.16.

[133] Vukusic, P, Wootton, RJ and Sambles, JR. 'Remarkable Iridescence in the Hindwings of the Damselfly Neurobasis Chinensis Chinensis (Linnaeus) (Zygoptera: Calopterygidae)'. Proceedings of the Royal Society of London B: Biological Sciences 271.1539 (2004), pp. 595–601. DOI: 10.1098/rspb.2003.2595. pmid: 15156917.

[134] Stavenga, DG, Giraldo, MA and Leertouwer, HL. 'Butterfly Wing Colors: Glass Scales of Graphium Sarpedon Cause Polarized Iridescence and Enhance Blue/Green Pigment Coloration of the Wing Membrane'. Journal of Experimental Biology 213.10 (2010), pp. 1731–1739. DOI: 10.1242/jeb.041434. pmid: 20435824.

[135] Yoshioka, S, Kinoshita, S, Iida, H and Hariyama, T. 'Phase-Adjusting Layers in the Multilayer Reflector of a Jewel Beetle'. Journal of the Physical Society of Japan 81.5 (2012), p. 054801. DOI: 10.1143/JPSJ.81.054801.

[136] Mouchet, SR, Lobet, M, Kolaric, B, Kaczmarek, AM, Van Deun, R et al. 'Photonic Scales of Hoplia Coerulea Beetle: Any Colour You Like'. Materials Today: Proceedings. The Living Light Conference (May 4 - 6) 2016, San Diego (USA) 4 (4, Part A 2017), pp. 4979–4986. DOI: 10.1016/j.matpr.2017.04.104.

[137] Ghate, E, Bhoraskar, SV and Kulkarni, GR. 'Study of Nano-Architecture of the Wings of Paris Peacock Butterfly'. In: Proc. SPIE 8598, Bioinspired, Biointegrated, Bioengineered Photonic Devices. SPIE BiOS. Ed. by Lee, LP, Rogers, JA and Yun, SH. Vol. 859805. San Francisco, 2013, p. 8. DOI: 10.1117/12.2003061.

[138] Gur, D, Leshem, B, Pierantoni, M, Farstey, V, Oron, D et al. 'Structural Basis for the Brilliant Colors of the Sapphirinid Copepods'. Journal of the American Chemical Society 137.26 (2015), pp. 8408–8411. DOI: 10.1021/jacs.5b05289.

[139] Piszter, G, Kertész, K, Bálint, Z and Biró, LP. 'Variability of the Structural Coloration in Two Butterfly Species with Different Prezygotic Mating Strategies'. PLOS ONE 11.11 (2016), e0165857. DOI: 10.1371/journal.pone.0165857.

[140] Pérez i de Lanuza, G and Font, E. 'Iridescent (Angle-Dependent Reflectance) Properties of Dorsal Coloration in Podarcis Muralis (Laurenti, 1768)'. Amphibia-Reptilia 37.4 (2016), pp. 441–445.

[141] Santos, SI, Lumeij, JT, Westers, P and van Wandelen, BB. 'Sexual Dichromatism in the European Magpie Pica Pica . Not as Black and White as Expected'. Ardea 95.2 (2007), pp. 299–310. DOI: 10.5253/078.095.0212.

[142] Kientz, B, Luke, S, Vukusic, P, Péteri, R, Beaudry, C et al. 'A Unique Self-Organization of Bacterial Sub-Communities Creates Iridescence in Cellulophaga Lytica Colony Biofilms'. Scientific Reports 6 (2016), p. 19906. DOI: 10.1038/srep19906.

[143] Liu, F, Yin, H, Dong, B, Qing, Y, Zhao, L et al. 'Inconspicuous Structural Coloration in the Elytra of Beetles Chlorophila Obscuripennis (Coleoptera)'. Physical Review E 77.1 (2008), p. 012901. DOI: 10.1103/PhysRevE.77.012901.

[144] Johansen, VE, Catón, L, Hamidjaja, R, Oosterink, E, Wilts, BD et al. 'Genetic Manipulation of Structural Color in Bacterial Colonies'. Proceedings of the National Academy of Sciences 115.11 (2018), pp. 2652–2657. DOI: 10.1073/pnas.1716214115. pmid: 29472451.

[145] Rutowski, RL, Nahm, AC and Macedonia, JM. 'Iridescent Hindwing Patches in the Pipevine Swallowtail: Differences in Dorsal and Ventral Surfaces Relate to Signal Function and Context'. Functional Ecology 24.4 (2010), pp. 767–775. DOI: 10.1111/j.1365-2435.2010.01693.x.

[146] Rutowski, RL and Rajyaguru, PK. 'Male-Specific Iridescent Coloration in the Pipevine Swallowtail (Battus Philenor) Is Used in Mate Choice by Females but Not Sexual Discrimination by Males'. Journal of Insect Behavior 26.2 (2013), pp. 200–211. DOI: 10.1007/s10905-012-9348-2.

[147] Noh, H, Liew, SF, Saranathan, V, Prum, RO, Mochrie, SGJ et al. 'Contribution of Double Scattering to Structural Coloration in Quasiordered Nanostructures of Bird Feathers'. Physical Review E 81.5 (2010), p. 051923. DOI: 10.1103/PhysRevE.81.051923.

[148] Wilts, BD, Pirih, P, Arikawa, K and Stavenga, DG. 'Shiny Wing Scales Cause Spec(Tac)Ular Camouflage of the Angled Sunbeam Butterfly, Curetis Acuta'. Biological Journal of the Linnean Society 109.2 (2013), pp. 279–289. DOI: 10.1111/bij.12070.